



HAL
open science

Toward a Rational Design of 3d-4f Heterometallic Coordination Polymers based on Mixed Valence Copper Centers

Carlos Cruz, Francisco Rubio, Diego Venegas-Yazigi, Nathalie Audebrand, Christophe Calers, Evgenia Spodine, Veronica Paredes-Garcia

► **To cite this version:**

Carlos Cruz, Francisco Rubio, Diego Venegas-Yazigi, Nathalie Audebrand, Christophe Calers, et al.. Toward a Rational Design of 3d-4f Heterometallic Coordination Polymers based on Mixed Valence Copper Centers. *Crystal Growth & Design*, 2019, 19 (12), pp.7055-7066. 10.1021/acs.cgd.9b00816 . hal-02438533

HAL Id: hal-02438533

<https://univ-rennes.hal.science/hal-02438533>

Submitted on 11 Feb 2020

HAL is a multi-disciplinary open access archive for the deposit and dissemination of scientific research documents, whether they are published or not. The documents may come from teaching and research institutions in France or abroad, or from public or private research centers.

L'archive ouverte pluridisciplinaire **HAL**, est destinée au dépôt et à la diffusion de documents scientifiques de niveau recherche, publiés ou non, émanant des établissements d'enseignement et de recherche français ou étrangers, des laboratoires publics ou privés.

1
2
3
4
5
6
7
8
9
10
11
12
13
14
15
16
17
18
19
20
21
22
23
24
25
26
27
28
29
30
31
32
33
34
35
36
37
38
39
40
41
42
43
44
45
46
47
48
49
50
51
52
53
54
55
56
57
58
59
60

Towards a Rational Design of $3d-4f$ Heterometallic Coordination Polymers based on Mixed Valence Copper Centers

*Carlos Cruz,^{a,b} Francisco Rubio^{a,b} Diego Venegas-Yazigi,^{b,c} Nathalie Audebrand,^d Christophe Calers,^d Evgenia Spodine^{b,e} and Verónica Paredes-García^{*a,b}*

^a Universidad Andrés Bello, Facultad de Ciencias Exactas, Departamento de Ciencias Químicas, Santiago, Chile.

^b CEDENNA, Santiago, Chile.

^c Universidad de Santiago de Chile, Facultad de Química y Biología, Departamento de Ciencias de los Materiales, Santiago, Chile

^d Univ Rennes, CNRS, ISCR (Institut des Sciences Chimiques de Rennes) - UMR 6226, F-35000 Rennes, France

^e Universidad de Chile, Facultad de Ciencias Químicas y Farmacéuticas, Departamento de Química Inorgánica y Analítica, Santiago, Chile.

ABSTRACT

In the present work we report two new Cu^I/Cu^{II}-Gd^{III} mixed valence heterometallic coordination polymers (HCP), [Gd(H₂O)₄Cu^{II}Cu^I(IDC)₂] **1** and [Gd₂(H₂O)₂(C₂O₄)₂Cu^{II}(IDC)₂Cu^I₂(4,4'-bipy)]·4.5H₂O **2** obtained under solvothermal synthesis using 1H-imidazole-4,5-dicarboxylic acid (H₃IDC) as principal *N,O*-bifunctional organic linker. In both compounds, the stabilization of the Cu^I cations is achieved only by the coordination of *N*-atoms belonging to the organic ligands. While, **1** presents a 2D honeycomb network obtained by the coordination of single organic linker (IDC³⁻), **2** contains three different organic ligands (IDC³⁻, C₂O₄²⁻ and 4,4'-bipy), which allow the construction of a 3D network. From a magnetic point of view, **1** and **2** behave as simple paramagnets at high temperature, presenting ferromagnetic interactions below 50 K, a positive magnetic coupling constant of $J = 0.60 \text{ cm}^{-1}$ and $J = 0.22 \text{ cm}^{-1}$ was obtained for **1** and **2** respectively. To the best our knowledge **1** and **2** correspond to the second and third reported examples containing a Cu^I/Cu^{II} mixed valence system assembled with Gd^{III} cations, thus enriching the chemistry involved in the *3d-4f* metal-organic materials.

KEYWORDS. Coordination Polymers, Copper, Gadolinium, Mixed-Valence, *3d-4f*, Magnetism

1. INTRODUCTION

In recent years coordination polymers (CP) have been widely studied in materials science due to their excellent chemical and physical properties, such as porosity, chemical and thermal stability and catalytic activity, making the rational design of new CP a continuous challenge for

1
2
3 researchers.^{1,2,3,4} In this sense, the combination of two different metal cations in the same
4
5
6 structure, such as first row transition (*3d*) and lanthanide (*4f*) cations has been used as a strategy
7
8
9 to obtain new CPs with novel structures and potential applications such as magnetic
10
11
12 refrigeration, solid state luminescence and catalysis.^{5,6,7,8,9,10} Compared with the lanthanide
13
14
15 series, first row transition metals have a richer chemistry as a consequence of the various
16
17
18 oxidation states (from +1 to +7) and coordination geometries. Specifically, Cu^I and Cu^{II} cations
19
20
21 can adopt a wide variety of coordination geometries (linear, trigonal, tetrahedral, trigonal
22
23
24 bipyramid, square base pyramid, octahedral) as compared to other transition metal ions. The
25
26
27 coordination plasticity of the copper cations to accommodate different amounts of donor atoms
28
29
30
31 has been also exploited in the construction of *3d-4f* extended structures.¹¹
32
33
34
35
36
37

38 From a magnetic point of view, Cu^{II} CPs have been widely studied due to the simple
39
40
41 paramagnetic ground state ($S=1/2$) of this cation, which allows magneto-structural
42
43
44 correlations.^{12,13} After Bencini et al.¹⁴ found a compound showing ferromagnetic coupling
45
46
47 phenomenon between Cu^{II} and Gd^{III}, great efforts have been made to obtain Cu^{II}-Ln^{III}
48
49
50
51 heterometallic compounds with higher dimensionality, seeking for new magnetic materials.¹⁵
52
53
54
55 Thus, Cu^{II}-Ln^{III} heterometallic networks have been reported in the last decade presenting
56
57
58
59
60

1
2
3 ferromagnetic behavior based on different *N,O*-bifunctional organic ligands, such as,
4
5
6 iminodiacetic acid,¹⁶ glycine,¹⁷ glycinehydroxamic acid,¹⁸ pyrazoledicarboxylic acid¹⁹ and
7
8
9 benzotriazolecarboxylic acid.²⁰
10
11

12
13 On the other hand, considering that the full shell of Cu^I ($3d^{10}$) can be used as an antenna to
14
15
16 improve lanthanide luminescence, Cu^I-Ln^{III} heterometallic coordination polymers (HCPs) have
17
18
19 been the focus of research in the solid state light emissive materials.^{21,22} Literature presents a
20
21
22 very rich Cu^I-Ln^{III} coordination polymer chemistry in which Cu^I is stabilized into extended
23
24
25 structures using principally functionalized *N*-heterocyclic ligands, such as pyridine and
26
27
28 pyrazine.^{23,24,25,26,27} For the majority of the reported Cu^I-Ln^{III} CP the stabilization of Cu^I is not
29
30
31 always done by the coordination of only a *N*-organic ligand, but also the presence of coordinated
32
33
34 halides anions is found.^{28,29,30,31,32,33,34}
35
36
37
38
39
40

41 To the best of our knowledge, the only example of a *3d-4f* HCP containing Cu^I/Cu^{II} has been
42
43
44 obtained by Luo et al. [Gd₂Cu^{II}₂Cu^I₅(IN)₁₀(μ₂-Cl)(μ₂-OH₂)₂(μ₃-OH)₂](ClO₄)₂ (HIN= isonicotinic
45
46
47 acid),³⁵ probably due to the coordination requirements of Cu^I, Cu^{II} and Ln^{III} cations present in
48
49
50 the same structure are not easily satisfied. Furthermore, considering the instability and the poor
51
52
53 solubility of the Cu^I compounds and the fact that usually compounds based on this cation are
54
55
56
57
58
59
60

1
2
3 obtaining for reduction of Cu^{II} cation, the possibility to have in the same structure Cu^I, Cu^{II} and
4
5
6 Ln^{III} cations it is a great challenge from a synthesis point of view.
7

8
9
10 In the present work, we report two novel mixed valence Cu^I/Cu^{II}-Ln^{III} HCP,
11
12 [Gd(H₂O)₄Cu^{II}Cu^I(IDC)₂] **1** and [Gd₂(H₂O)₂(C₂O₄)₂Cu^{II}(IDC)₂Cu^I₂(4,4'-bipy)]·4.5H₂O **2**, obtained
13
14
15 using 1H-imidazole-4,5-dicarboxylic acid (H₃IDC) as the principal *N,O*-bifunctional organic
16
17 linker. H₃IDC has been already used by our research group, proving to be an excellent ligand to
18
19
20 obtain new *3d-4f* compounds, giving rise to HCP including a 2D Cu^{II}-Gd^{III} network,³⁶ Co^{II}-Gd^{III}
21
22
23 3D frameworks³⁷ and recently two *3d-Ce^{III}* compounds (*3d* ≠ Cu^{II}, Co^{II}).³⁸ In the present work,
24
25
26 two new HCP were prepared under solvothermal conditions. **1** presents a 2D structure showing
27
28
29 a honeycomb type arrangement, while **2** corresponds to a 3D structure. Structural, thermal
30
31
32 stability, spectroscopic and magnetic properties are discussed in detail.
33
34
35
36
37
38
39
40

41 2. EXPERIMENTAL SECTION

42
43
44 All reagents and solvents used to obtain **1** and **2** were of p.a. quality and were used without
45
46
47 any previous purification. Figure 1, summarizes the synthesis of the two compounds.
48
49
50

51 2.1. Synthesis of [Gd(H₂O)₄Cu^{II}Cu^I(IDC)₂] **1**

1
2
3 A mixture of $\text{Cu}(\text{NO}_3)_2 \cdot 3\text{H}_2\text{O}$ (0.5 mmol), Gd_2O_3 (0.13 mmol), H_3IDC (0.5 mmol) and
4
5
6 $\text{H}_2\text{C}_2\text{O}_4 \cdot 2\text{H}_2\text{O}$ (0.5 mmol) in 14 mL of H_2O and 1 mL of ethanol (EtOH) was treated with 80 μL
7
8
9 (0.6 mmol) of triethylamine (TEA). The resultant mixture was placed in a 23 mL Teflon-lined
10
11
12 stainless-steel autoclave vessel and heated at 165 °C under self-generated pressure for 4 days.
13
14
15
16
17 Finally, the reaction vessel was cooled down to room temperature at 3°C/h rate (48 hours); olive-
18
19
20 green needle-like crystals of **1**, suitable for X-ray diffraction, were separated by filtration.
21
22
23
24 Although oxalic acid is not present in the final product, without the addition of this reagent **1** is
25
26
27 not obtained. MW: 662.59 g/mol. Yield of 62%, based on the lanthanide salt. Calculated analysis
28
29
30 for $\text{Cu}_2\text{GdC}_{10}\text{H}_{10}\text{N}_4\text{O}_{12}$ (%): C, 18.13%; H, 1.52%; N, 8.46%. (%) Found: C, 18.76%; H, 1.56%;
31
32
33
34 N, 7.72%.

35 36 37 2.2. Synthesis of $[\text{Gd}_2(\text{H}_2\text{O})_2(\text{C}_2\text{O}_4)_2\text{Cu}^{\text{II}}(\text{IDC})_2\text{Cu}^{\text{I}}_2(4,4'\text{-bipy})] \cdot 4.5\text{H}_2\text{O}$ **2**

38
39
40
41 **2** was obtained using the same procedure as that of synthesis of **1** but adding 4,4'-bipyridine
42
43
44 (0.5 mmol) to the mixture; olive-green prismatic crystals of **2**, suitable for X-ray diffraction were
45
46
47 mechanically separated from the reaction medium. MW: 1260.68 g/mol. Yield: 13%, based on
48
49
50 the lanthanide salt. Calculated analysis for $\text{Cu}_3\text{Gd}_2\text{C}_{24}\text{H}_{23}\text{N}_6\text{O}_{22.5}$ (%): C, 22.86; H, 1.84; N, 6.67.
51
52
53
54
55 (%) Found: C, 22.52; H, 1.76; N, 7.06.
56
57
58
59
60

2.3. X-ray Data Collection and Structure Determination

Single-crystal X-ray diffraction data of compound **1** and **2** were collected at 150 K on a D8 VENTURE Bruker AXS diffractometer and processed with the APEX3 program suite,³⁹ using Mo-K α as X-ray wavelength. Frame integration and data reduction were carried out with the program SAINT,⁴⁰ and SADABS was employed for multiscan-type absorption corrections.⁴¹

Using the Olex2⁴² package, the structures were solved with the ShelXT⁴³ structure solution program using Dual Space Methods and refined with the ShelXL⁴⁴ refinement package, using least squares minimization based on F^2 . Crystallographic data, details on data collections and refinement parameters of the crystal structure are summarized in Table 1. Structure drawings have been made with TOPOs software.⁴⁵ Additional data concerning the crystals and the refinement parameters are detailed in the supporting information (Table S1).

All hydrogen atoms were properly localized, except the one belonging to O4W in **1** and O1W, O2W, O3W, O4W and O9 in **2**. Nevertheless, all hydrogen atoms were considered in the final formula. Additionally, crystallization H₂O molecules O1W, O2W, O3W and O4W located into the interstitial spaces of **2** present disorder and were modelled by parts, giving a total amount of four

1
2
3 water molecules per unity of complex. The amount of H₂O of crystallization in the bulk material
4
5
6 was obtained experimentally using thermogravimetric analysis.
7
8

9
10 *In situ* temperature-dependent X-ray diffraction (TDXD) was performed for **1** in a flux of N₂ with
11
12 a Malvern Panalytical Empyrean powder diffractometer, using a germanium incident-beam
13
14 graphite monochromator, selecting the radiation Cu K α ₁, and a PIXcel 3D detector and equipped
15
16 with an Anton Paar HTK1200 oven chamber. *In situ* measurements were carried out at various
17
18 constant temperatures from ambient temperature until 800°C. Between each measurement
19
20 step, the sample was heated at a rate of 1.0 °C min⁻¹ to the desired temperature. Diffraction
21
22 patterns were collected over the angular range 5–60°(2 θ) with a counting time of 40 s step⁻¹ and
23
24 with a step length of 0.013°(2 θ).
25
26
27
28
29
30
31
32
33
34
35
36

37 38 2.4. Magnetic Measurements 39

40
41 Magnetic measurements were carried out using a Quantum Design Dynacool Physical Properties
42
43 Measurement System (PPMS), equipped with a Vibrating Sample Magnetometer (VSM). The *dc* data
44
45 were collected under an external applied field of 1 kOe in the 1.8–300 K temperature range.
46
47
48 Isothermal magnetizations were performed between 0 and \pm 90 kOe at temperatures varying
49
50
51 from 1.8 to 8 K. All Magnetic measurement were performed under crystalline power samples in
52
53
54
55
56
57
58
59
60

1
2
3 plastic sampleholder. Diamagnetic corrections (estimated from Pascal constants) were
4
5
6 considered.⁴⁶
7

8 9 10 2.5. Thermogravimetric analysis

11
12
13 Thermogravimetric analysis was performed on a Mettler Toledo TGA/DSC STAR system. The
14
15
16 samples were introduced in an alumina holder and heated under a N₂ atmosphere from room
17
18
19 temperature to 900 °C with a heating rate of 5 °C/min.
20
21
22

23 24 2.6. Spectroscopic measurements

25
26
27 UV–Vis–NIR spectra were obtained on a Perkin Elmer Lambda 1050 spectrophotometer UV–
28
29
30 Vis/NIR, equipped with a Perkin Elmer 150 mm InGaAs Integrating sphere. The measurements
31
32
33 were carried out in the 200–1200 nm range using the solid sample without any support.
34
35
36

37 38 3. RESULTS AND DISCUSSION

39
40
41 *3.1 Structural Characterization of [Gd(H₂O)₄Cu^{II}Cu^I(IDC)₂] 1 and*
42
43
44 *[Gd₂(H₂O)₂(C₂O₄)₂Cu^{II}(IDC)₂Cu^I₂(4,4'-bipy)]·4.5H₂O 2*
45
46
47

48 X-ray diffraction analysis reveals that compound **1** crystallizes in the $P\bar{1}$ triclinic space group,
49
50
51 presenting an asymmetrical unit with two different copper (Cu^I, Cu^{II}) and one gadolinium cations,
52
53
54
55 four water molecules and two independent fully deprotonated IDC³⁻ species. Both IDC³⁻ anions
56
57
58
59
60

1
2
3 bind two copper and one gadolinium cations, at the same time presenting a $\eta^3\text{-}\kappa\text{N}\text{-}\kappa\text{O}',\text{O}''\text{-}\kappa\text{O}''',\text{N}'$
4
5
6 coordination mode (Figure 2a). Cu1 cations are bonded to two IDC³⁻ anions, which are
7
8
9
10 connected in a monodentate mode through N atoms with a *trans* conformation, with bond
11
12
13 distances of Cu1-N2=1.872(2) Å and Cu1-N3=1.880(2) Å. Cu1 is also weakly interacting with
14
15
16 the two carboxylates groups belonging to each IDC³⁻ ligand with Cu-O bond distances of Cu1-
17
18
19 O=2.576(2) Å and 2.781(2) Å (Figure 3a). Meanwhile, Cu2 cations present a coordination
20
21
22 environment formed by two IDC³⁻ anions (Figure 3b) bonded by N-imidazole and O-carboxylate,
23
24
25 forming two independent NCCO five member rings, with bond distances of Cu2-N1=1.933(2) Å,
26
27
28 Cu2-N4=1.922(2) Å, Cu2-O1=1.973(2) Å, Cu2-O5=1.976(2) Å and N-Cu-O angles of 98.99(9)°
29
30
31 (N1-Cu2-O5) and 82.44(9)° (N4-Cu2-O5). Taking into account the bond distance for both
32
33
34 copper cations, Cu1 should be better described with a CuN₂ environment, having a linear
35
36
37 geometry with a N-Cu-N angle of 177.28(1)°. In the case of Cu2, the cation can be well described
38
39
40
41 with a CuN₂O₂ environment presenting a distorted square plane geometry, since the Cu-O and
42
43
44 Cu-N bond distances are comparable in length, and N-Cu-O angles are close to 90°.
45
46
47
48 Furthermore, comparing the bond distances and coordination geometries of the two types of
49
50
51
52 copper cations, it is possible to infer that Cu1 should present a 1+ oxidation state, while Cu2
53
54
55
56
57
58
59
60

1
2
3 must present a 2+ oxidation state, which is in perfect agreement with the charge balance of the
4
5
6 framework.
7

8
9
10 On the other hand, Gd1 presents a GdO₈ coordination sphere, with Gd-O bond distances in
11
12
13 the range of 2.558(2)-2.260(2) Å, formed by two κO',O''IDC³⁻ species, bonded by two O-
14
15
16 carboxylate atoms generating two independent seven member rings. The coordination around
17
18
19 Gd^{III} cations is completed by four H₂O molecules (Figure 3c), leading to a bicapped trigonal
20
21
22
23
24 prism geometry, corroborated by a continuous shape measurement using the SHAPE
25
26
27 software.⁴⁷
28
29

30
31 Furthermore, **1** presents a honeycomb topology formed by heterometallic [Gd₂Cu^I₂Cu^{II}₂]
32
33
34 hexagonal moieties (Figure 4a). Each corner of the [Gd₂Cu^I₂Cu^{II}₂] hexagon is formed by an IDC³⁻
35
36
37 anion connected to each other by one Gd^{III} and one copper cation (Cu^I or Cu^{II}), forming an
38
39
40 alternating Gd^{III}-Cu^{II}-Cu^I ordering. The hexagonal honeycomb topology is shown more clearly in
41
42
43
44 a simplified structure in figure 4b, in which it is easy to see how the cations Cu^I, Cu^{II} and Gd^{III}
45
46
47 are behaving as linear nodes, while the IDC³⁻ linker can be defined as a tritopic trigonal plane
48
49
50 spacer. Moreover, it is interesting to note how of the H-bonding produced by the H₂O molecules
51
52
53
54 coordinated to Gd cation are the key of the resulting crystal packing of the layers. In this sense
55
56
57
58
59
60

1
2
3 if we only consider the arrangement of the four water molecules around of Gd^{III} belonging to one
4
5
6 layer, it is possible to observe how this disposition produces two types of interaction between
7
8
9 the adjacent layers. Thus, the three water molecules forming a tripod are localized in such way
10
11
12 that they are inserted in the hexagons of the cavity of one adjacent layer (Figure 4c), interacting
13
14 by H-bonding with the carboxylate groups of IDC³⁻ (Table 2 for H-bonding). This interaction
15
16
17 produces a displaced-layer stacking, with each hexagonal cavity filled by a water-tripod avoiding
18
19
20 the existence of porosity in the structure, defining a double-layer arrangement. Furthermore, the
21
22
23 last H₂O molecule coordinating the Gd^{III} cations is pointing just opposite to the former water-
24
25
26 tripod, allowing a second H-bond interaction between the double-layers (Table 2 for H-bonding),
27
28
29 giving the final crystal packing (Figure 4d).
30
31
32
33
34
35
36
37

38 Since Cu1 and Cu2 cations have an unsaturated coordination sphere (linear and square plane
39
40 respectively) in the 2D structure of [Gd(H₂O)₄Cu^{II}Cu^I(IDC)₂] **1**, this heterometallic compound is
41
42
43 a good candidate as starting material to generate a 3D coordination polymer using a linear ligand
44
45
46 such as 4,4'-bipyridine as interlayer linker (two step synthesis). However, by adding the 4,4'-
47
48
49 bipyridine ligand in the same reaction media used for **1** (one pot synthesis) a new compound **2**
50
51
52
53
54
55
56
57
58
59
60

1
2
3 was formed. This compound is also a Cu^I-Cu^{II}-Gd^{III} mixed valence HCP, but now presenting a
4
5
6 3D network [Gd₂(H₂O)₂(C₂O₄)₂Cu^{II}(IDC)₂Cu^I₂(4,4'-bipy)]·4.5H₂O.
7
8

9
10 Compound **2** crystallizes in the $P\bar{1}$ triclinic space group and presents a 3D coordination
11
12 framework, with an asymmetrical unit formed by one and a half copper and one gadolinium
13
14 cations, one water molecule, one independent fully deprotonated IDC³⁻ species, one oxalate
15
16 anion (C₂O₄²⁻) and half 4,4'-bipyridine (4,4'-bipy). Additionally, the compound also presents
17
18 disordered crystallization H₂O molecules. The coordination mode of the IDC³⁻ species is the
19
20 same as the one observed in **1**, $\eta^3\text{-}\kappa N\text{-}\kappa O', O''\text{-}\kappa O''', N'$ (Figure 2a). The 4,4'-bipy molecule serves
21
22 as a ditopic ligand, connecting two copper centers in a $\mu_2\text{-}\kappa N\text{-}\kappa N'$ coordination fashion, while the
23
24 C₂O₄²⁻ anions coordinate Gd^{III} in $\mu_2\text{-}O, O'\text{-}\kappa O'', O'''$ mode (Figure 2b-c). Similarly, as in **1**, to
25
26 achieve the electron neutrality of the network and balance the negative charge belonging to
27
28 IDC³⁻ and C₂O₄²⁻ species **2** must present copper cations in two different oxidation states. Cu1
29
30 presents a CuN₂O₂ environment formed by two IDC³⁻ anions (Figure 5a) coordinated by N-
31
32 imidazole and O-carboxylate, forming two NCCO five-member rings, with Cu1-O1=1.962(3) Å
33
34 and Cu1-N=Å, Cu1-N1=1.915(3) Å bond length distances. Moreover, since the N-Cu-O angles
35
36 are near to 90° (N1-Cu1-O1=96.01(12)°, N1-Cu1-O1=83.99(12)°), the geometry around Cu1
37
38
39
40
41
42
43
44
45
46
47
48
49
50
51
52
53
54
55
56
57
58
59
60

1
2
3 can be well defined as square planar. On the other hand, Cu2 is bonded to one IDC³⁻ anion and
4
5
6 one 4,4'-bipy, connected by means of nitrogen atoms, presenting Cu2-N2=1.846(3) Å, Cu2-
7
8
9 N3=1.852(3) Å bond lengths. Cu2 is also weakly interacting with one carboxylate group
10
11
12 belonging to IDC³⁻ with a distance of Cu2-O4=2.627(2) Å (Figure 5b). Furthermore, the N2-Cu2-
13
14
15 N3 angle is 178.71(14)°, while the N-Cu2-O4 is 105.58(12)° and 74.87(10)°; therefore the
16
17
18 environment around Cu2 can be defined as lineal CuN₂.
19
20
21
22
23

24 Considering the type of coordination environment, Cu1 can be assigned a 2+ oxidation state
25
26
27 with a square planar geometry, while Cu2 presents a 1+ oxidation state with linear geometry.
28
29
30
31 Meanwhile, Gd1 presents a GdO₉ environment formed by two IDC³⁻ molecules coordinated by
32
33
34 one ($\kappa O, O'$ IDC³⁻) and two ($\kappa O', O''$ IDC³⁻) carboxylate groups. Also, two $\kappa O, O'-\kappa O'', O'''$ -C₂O₄²⁻
35
36
37 anions and one H₂O molecules are bonded to Gd1 centers with Gd-O bond distance in the range
38
39
40 of 2.547(2)-2.387(2) Å, leading to a capped square antiprism geometry, corroborated by an
41
42
43 continuous shape measurement using the SHAPE software (Figure 5c).⁴⁷
44
45
46
47
48

49 Moreover, the 3D extended structure of **2** can be disassembled in two different homometallic
50
51
52 substructures. The first one corresponding to a cationic 1D substructure formed by
53
54
55 [Gd₂(H₂O)₂(C₂O₄)₂]²⁺ building units, in which the Gd^{III} centers are bridged by two different oxalate
56
57
58
59
60

1
2
3 anions (Figure 6a) forming a zigzag chain along *c* axis. Meanwhile, the second substructure
4
5
6 corresponds to anionic mixed valence Cu^I/Cu^{II} linear chains, formed by [Cu^{II}(IDC)₂Cu^I₂(4,4'-
7
8
9 bipy)]²⁻ as building units (Figure 6b). Figure 6c depicts the cross-linked connectivity between
10
11
12 both homometallic substructures, showing clearly the role of the IDC³⁻ anion in the assembly of
13
14
15 both homometallic chains. The IDC³⁻ anion of the Cu^I/Cu^{II} chains anchors Gd^{III} centers of two
16
17
18 adjacent [Gd₂(H₂O)₂(C₂O₄)₂]²⁺ chains, with a $\kappa O, O'$ -IDC³⁻ coordination fashion, generating the
19
20
21 3D framework. As stated in the introduction section, the unique example of a *3d-4f* mixed
22
23
24 valence compound is [Gd₂Cu^{II}₂Cu^I₅(IN)₁₀(μ_2 -Cl)(μ_2 -OH)₂(μ_3 -OH)₂](ClO₄)₂, which was
25
26
27 synthesized by hydrothermal reaction of isonicotinic acid (HIN) as bifunctional ligand, Gd₂O₃ and
28
29
30 CuCl₂ as metal precursors in the presence of HClO₄ and (NH₄)HCOO, giving a 3D structure
31
32
33 constructed by the self-assembly of 12-connected Gd^{III}₂Cu^{II}₂ subunits interconnected by Cu^I-IN-
34
35
36 fragments.³⁵ In the case of **1** and **2**, the inclusion of a Cu^I/Cu^{II} mixed-valence compound was
37
38
39 also achieved by the partial hydrothermal reduction of a cupric salt precursor. Furthermore, it
40
41
42 has been reported by Truong et al. that under hydrothermal condition oxalic acid can act as
43
44
45 reducing agent; therefore, this reactive could be the responsible for the reduction of copper salt
46
47
48 under autogenerated pressure. This could be related with the fact that if oxalic acid is not present
49
50
51
52
53
54
55
56
57
58
59
60

1
2
3 as reagent in the corresponding synthesis, **1** and **2** were not obtained. Moreover, Truong et al.
4
5
6 propose that oxalic acid degrades to carbon monoxide or carbon dioxide and that a copper oxalate
7
8
9 complex act as intermediate in the Cu^I/Cu^{II} reduction process.⁴⁸ Another interesting feature in
10
11
12 the compound reported by Luo et al. is the presence of Cu^I centers in linear CuO₂ and CuN₂
13
14
15 environment, similar to that of **2**. Linear conformations are common in other d¹⁰ coordination
16
17
18 polymers such as Au^I^{49,50} and Ag^I,^{51,52} however Cu^I is usually reported presenting trigonal^{53,54}
19
20
21 and tetrahedral^{55,56} geometries, while Cu^I/Cu^{II} and Cu^I CPs containing linear Cu^I are more
22
23
24 scarce.⁵⁷ On the other hand, according to the Robin and Day classification, **1** and **2** can be
25
26
27 described as Class I mixed valence compounds, since in both structures the Cu^I and Cu^{II} cations
28
29
30 can be identified by the difference in their coordination geometries.^{58,59}
31
32
33
34
35
36
37

38 Additionally, another structural comparison can be made between **1** and two 3D frameworks
39
40
41 $\{[\text{Zn}_3(\text{IDC})_2(4,4'\text{-bipy})_3]\cdot(4,4'\text{-bipy})\cdot 8\text{H}_2\text{O}\}_n$ obtained by Lu et al.⁶⁰ and $\{[\text{Co}_3(\text{IDC})_2(4,4'\text{-}$
42
43
44 $\text{bipy})_3]\cdot 6\text{H}_2\text{O}\cdot \text{DMF}\}_n$ obtained by Wang et al.⁶¹ It is quite surprising that although these both
45
46
47 frameworks are constructed only by M^{II} cations (M^{II} = Zn^{II} and Co^{II}), presents $[\text{M}_3(\text{IDC})_2]_n$ 2D
48
49
50 sub-structures with exactly the same honeycomb topology as the one observed in **1**. In both
51
52
53 cases, the layers are formed by M^{II} cations, connected through alternating imidazolate $\mu_2\text{-}\kappa N, N'$
54
55
56
57
58
59
60

1
2
3 IDC³⁻ and *anti-anti* μ_2 - κ O,O'-IDC³⁻ carboxylate, which are further pillared by μ_2 -N,N'-4,4'-bipy
4
5
6 connections, presenting hexagonal cavities into the 3D CP. This fact suggests that the property
7
8
9 of generate 2D structures with honey comb topology is an intrinsic property of the IDC³⁻ ligands,
10
11
12 being independent of the metal ions used.
13
14
15

16
17 *3.2 Thermal stability of [Gd(H₂O)₄Cu^{II}Cu^I(IDC)₂] 1 and [Gd₂(H₂O)₂(C₂O₄)₂Cu^{II}(IDC)₂Cu^I₂(4,4'-*
18
19 *bipy)]·4.5H₂O 2*
20
21
22

23
24 Thermogravimetric analysis between 25 and 900°C under N₂ atmosphere was performed to
25
26
27 characterize the thermal stability of **1** and **2** (inset Figure 7). Thermogram of **1** shows two
28
29
30 consecutive weight losses, between 95-220° (7.56 wt%) and 220-290°C (2.75 wt%) attributed
31
32
33 to the release of the four coordinated water molecules (10.3 wt%). After these two steps, a third
34
35
36 weight loss of 27.9% is observed from 350° C, indicating the thermal decomposition of the
37
38
39 framework. On the other hand, **2** presents a first weight loss between 40-210 °C with a value of
40
41
42 6.38 wt%, which can be associated to the thermal outflow of the 4.5 crystallization H₂O
43
44
45 molecules, occluded in the interstices of the 3D structure of **2**. The percentage associated with
46
47
48 this weight loss is a little higher than the obtained from X-ray diffraction analysis (4.0 H₂O
49
50
51 molecules). Later, three consecutive smooth weight losses are observed between 210° and
52
53
54
55
56
57
58
59
60

1
2
3 330°C with a total percentage of 39.17 wt%, associated with the thermal decomposition of the
4
5
6 framework. The stability of this type of networks can be associated to the hydrogen bonding
7
8
9 interactions between the water molecules and carboxylate oxygen atoms belonging to organic
10
11
12 linkers, stabilizing significantly the network packing,^{62,63,64} Furthermore, in 3D frameworks the
13
14
15 guest molecule evacuation from interstitial cavities can be accompanied by collapse of the
16
17
18 structure of the extended networks.^{65,66}
19
20
21
22
23

24 *In situ* temperature-dependent X-ray diffraction (TDXD) was performed for the **1** framework to
25
26
27 establish structural correlations with TG analysis (Figure 7). Comparing the experimental **1**
28
29
30 powder diffractogram with the calculated pattern from single crystal (Figure S1), it is clear that
31
32
33 the **1** powder phase is pure. Unfortunately, it was not possible to perform the TDXD of **2**, due to
34
35
36 the low yield in the synthesis of this compound.
37
38
39
40

41 When **1** is heated from room temperature to 290°C under N₂ atmosphere, TDXD experiments
42
43
44 show that the diffraction pattern is maintained, proving that the release of the coordination H₂O
45
46
47 molecules does not affect the structural integrity of **1**. Until 300°C no changes are registered in
48
49
50 TDXD, showing that the framework is stable even after the dehydration process. From 300°C to
51
52
53 350°C the principal diffraction peaks of **1** begin to disappear. Considering that the TG analysis
54
55
56
57
58
59
60

1
2
3 shows a non-significant weight loss in this temperature range, the loss of the crystallinity process
4
5
6 can be suggested. Moreover, above 450°C new peaks start to appear at higher 2θ values,
7
8
9 indicating that new crystalline phases are formed. The peaks position at 43.3° and 50.4° correlate
10
11
12 well with (111) and (200) diffraction planes of metallic Cu⁰ phase (ICDD PDF2 No. 01-089-
13
14 2838),^{67,68} indicating that the reduction of Cu^I/Cu^{II} cations to *fcc*-Cu⁰ is taking place. Starting
15
16
17 from 650°C, new peaks at 28.6°, 33.1° and 47.5° can be associated to the (222), (400) and (440)
18
19
20
21
22
23
24 diffraction planes of cubic-Gd₂O₃ (ICDD PDF2 No. 03-065-3181).⁶⁹
25
26

27 *3.3 Spectroscopic characterization*

28
29
30
31 UV-Vis-NIR electronic spectra are interesting to complement the characterization of **1** and **2**.
32
33
34 Cu^{II} complexes show *d-d* absorption bands in the Vis-NIR range, while the complete *3d* shell in
35
36
37 Cu^I compounds prevents metal-centered electronic transitions. At the same time, Cu^I
38
39
40
41 compounds may present metal to ligand charge transfer (MLCT), which are generally more
42
43
44
45 intense and at higher energies as compared to the *d-d* transitions.⁷⁰ Figure S2 shows the solid
46
47
48
49 state UV-Vis-NIR spectra of both compounds in the region between 200 and 850 nm. A broad
50
51
52
53 band covering almost all the studied region is observed in both spectra. At lower wavelengths,
54
55
56
57
58
59
60 a band centered near 260 nm can be associated to a ligand-centered absorption, belonging to

1
2
3 the organic species.⁷¹ At higher wavelengths, a band centered at 582 and 535 nm for **1** and **2**,
4
5
6 respectively can be related with the overlapping of the three spin allowed *d-d* transitions of Cu^{II}
7
8
9
10 centers in a square planar geometry, $d_{xz}/d_{yz} \rightarrow d_{x^2-y^2}$, $d_{z^2} \rightarrow d_{x^2-y^2}$ and $d_{xy} \rightarrow d_{x^2-y^2}$.⁷² An
11
12
13 additional band can be observed at 376 and 395 nm for **1** and **2** associated to metal to ligand
14
15
16 charge transfer between Cu^I centers and the heterocyclic organic ligands.⁷³ These results also
17
18
19
20 permit to corroborate the existence of a mixed-valence Cu^I/Cu^{II} system in **1** and **2**.
21
22
23

24 In compound **1** and **2**, two separate emission process could be expected, one of them in the
25
26
27 UV region corresponding to a *f-f* transition belonging of Gd^{III} cation,⁷⁴ and the other one an
28
29
30 emission of the Cu^I-ligand fragment which should appear in the visible region.^{21,22} To explore
31
32
33
34 the luminescence properties of **1** and **2**, solid state emission spectra were recorded at room
35
36
37 temperature using as excitation the energy maxima observed in the absorption spectra.
38
39
40
41 Nevertheless, no emission was observed at the studied conditions. These results could be
42
43
44 related with the fact that in **1** and **2** the *f*-excited states of Gd^{III} are above of the excited state of
45
46
47 the organic ligand, inhibiting a possible ligand→Gd antenna effect.^{75,76} On the other hand, the
48
49
50
51 Cu^{II} cations in **1** and **2** could be acting as a quencher of the Cu^I-ligand emission, since the
52
53
54
55
56
57
58
59
60

1
2
3 divalent copper cation presents a broad intense $d-d$ absorption band in the Vis-NIR regions,
4
5
6 which can deactivate emissive excited states in non-radiative pathways.⁷⁷
7

8 9 10 *3.4 Magnetic Properties*

11
12
13 Figure 8 shows $\chi_m T$ vs T plots for $[\text{Gd}(\text{H}_2\text{O})_4\text{Cu}^{\text{II}}\text{Cu}^{\text{I}}(\text{IDC})_2]$, **1** and
14
15
16
17 $[\text{Gd}_2(\text{H}_2\text{O})_2(\text{C}_2\text{O}_4)_2\text{Cu}^{\text{II}}(\text{IDC})_2\text{Cu}^{\text{I}}_2(4,4'\text{-bipy})]\cdot 4.5\text{H}_2\text{O}$ **2** between 300-1.8 K at 1 kOe. The $\chi_m T$
18
19
20 value observed at 300 K for **1** and **2** is 8.4 and 16.0 emu K mol⁻¹ respectively, which is close to
21
22
23 the expected value for non-interacting paramagnetic centers in both frameworks. For **1** a value
24
25
26 of 8.25 emu K mol⁻¹ should be expected for one Cu^{II} and one Gd^{III} cations, while in the case of
27
28
29
30
31 **2** a value of 16.13 emu K mol⁻¹ is expected for one Cu^{II} and two Gd^{III} cations, considering for
32
33
34 both compounds a $S_{\text{Cu}(\text{II})}=1/2$, $S_{\text{Gd}(\text{III})}=7/2$ and $g_{\text{Cu}/\text{Gd}}=2.0$. **1** and **2** show a constant $\chi_m T$ value till
35
36
37 50 K, indicating that a paramagnetic behavior is predominant in this temperature range.
38
39
40
41 Nevertheless, below 50 K an abrupt increase of the $\chi_m T$ values was observed for both
42
43
44
45 compounds, reaching a value of 13.06 and 19.46 emu K mol⁻¹ for **1** and **2**, respectively at 1.8 K,
46
47
48 indicating that a ferromagnetic behavior is displayed.
49

50
51
52 Additionally, field dependence of magnetization at 1.8, 3, 5 and 8 K represented as N_B vs H is
53
54
55 shown in Figure 9 for **1** and **2**. In both cases, the magnetization increases rapidly reaching a
56
57

1
2
3 plateau of $8 \mu_B$ at 40 kOe for **1** and $15 \mu_B$ at 50 kOe for **2**, being consistent with the saturation
4
5
6 values expected for the eight unpaired electrons of a core of $\text{GdCu}^{\text{II}}\text{Cu}^{\text{I}}$ and fifteen unpaired
7
8
9 electrons of a core of $\text{Gd}_2\text{Cu}^{\text{II}}\text{Cu}^{\text{I}}_2$.

11
12
13 Since both **1** and **2** are extended structures, the connectivity of the spin carriers is the key for
14
15
16 the magnetic behavior analysis, i.e. to define the proper magnetic network. In the case of **1**, the
17
18
19 structure can be reduced to $\text{Cu}^{\text{II}}\text{-Gd}^{\text{III}}$ chains linked through an *anti-anti* carboxylate bridge,
20
21
22 where the Cu-Gd-chains are interconnected by Cu^{I} diamagnetic centers. However, the lack of
23
24
25 an analytical model to fit the experimental magnetic data for a regular Cu-Gd ferromagnetic
26
27
28 chain, forces to use a simpler model to quantify the magnetic interaction between both cations.
29
30
31 In this sense, considering the isotropic character of the Cu^{II} and Gd^{III} cations the magnetic data
32
33
34 were analyzed using the spin-only Hamiltonian $\hat{H} = -2J\hat{S}_{\text{Cu}}\hat{S}_{\text{Gd}}$, which describes the super-
35
36
37 exchange interaction between one Cu^{II} and one Gd^{III} cation. Assuming that Cu^{II} and Gd^{III} have
38
39
40 equal g values, the experimental data can be fitted with the following analytical expression^{78,79}
41
42
43
44
45
46
47
48
49
50
51
52
53
54
55
56
57
58
59
60

$$\chi^m T = \frac{4Ng^2\beta^2 T}{kT} \left(\frac{7 + 15e^{\left(\frac{8J}{kT}\right)}}{7 + 9e^{\left(\frac{8J}{kT}\right)}} \right)$$

Where N is the Avogadro number, g is the Lande factor, β is the Bohr magneton, k is the Boltzmann constant and J is the coupling constant. The best fit of the parameters was obtained using a $J=0.60 \text{ cm}^{-1}$ and $g= 2.02$, with an agreement factor $R=4\times 10^{-3}$ ($R=\frac{\sum(\chi_m T_{\text{obs}})-(\chi_m T_{\text{exp}})^2}{\sum(\chi_m T_{\text{obs}})^2}$).

In the case of **2**, the compound presents a higher structural dimensionality, where the Cu^{II} and Gd^{III} spin carriers are bridged by a carboxylate anion and both Gd-Gd interactions can be produced by carboxylate or oxalate anions. However, it has been previously reported that due to the internal nature of the $4f$ electrons, the $\text{Gd}^{\text{III}}\text{-Gd}^{\text{III}}$ magnetic interaction are sufficient small to be neglected.^{80,81} Therefore, the magnetic network can be reduced to a more simple model considering only the interaction $\text{Cu}^{\text{II}}\text{-Gd}^{\text{III}}$ hetero-spins carriers.¹⁵ From a magnetic point of view, the extended 3D crystal network of **2** can be described as a linear trinuclear $\text{Gd}^{\text{III}}\text{-Cu}^{\text{II}}\text{-Gd}^{\text{III}}$ core, with $\text{Gd}^{\text{III}}\text{-Cu}^{\text{II}}$ centers connected through an *anti-anti* carboxylate bridge. This model leads to a spin-only Hamiltonian of $\hat{H} = -2J\hat{S}_{\text{Gd}1}\hat{S}_{\text{Cu}} - 2J\hat{S}_{\text{Cu}}\hat{S}_{\text{Gd}2}$, which gives rise to the following analytical expression⁸²

$$\chi_m T = \frac{Ng^2\beta^2 T A A}{2kT B B}$$

$$\begin{aligned}
 AA &= 1 + 10e^{\left(\frac{J}{kT}\right)} + e^{\left(-\frac{2J}{kT}\right)} + 35e^{\left(\frac{2J}{kT}\right)} + 10e^{\left(-\frac{3J}{kT}\right)} + 84e^{\left(\frac{3J}{kT}\right)} + 35e^{\left(-\frac{4J}{kT}\right)} + 165e^{\left(\frac{4J}{kT}\right)} + 84e^{\left(-\frac{5J}{kT}\right)} \\
 &\quad + 286e^{\left(\frac{5J}{kT}\right)} + 165e^{\left(-\frac{6J}{kT}\right)} + 84e^{\left(\frac{6J}{kT}\right)} + 286e^{\left(-\frac{7J}{kT}\right)} + 680e^{\left(\frac{7J}{kT}\right)} + 455e^{\left(-\frac{8J}{kT}\right)} \\
 BB &= 2 + 4e^{\left(\frac{J}{kT}\right)} + 2e^{\left(-\frac{2J}{kT}\right)} + 6e^{\left(\frac{2J}{kT}\right)} + 4e^{\left(-\frac{3J}{kT}\right)} + 8e^{\left(\frac{3J}{kT}\right)} + 6e^{\left(-\frac{4J}{kT}\right)} + 10e^{\left(\frac{4J}{kT}\right)} + 8e^{\left(-\frac{5J}{kT}\right)} + 12e^{\left(\frac{5J}{kT}\right)} \\
 &\quad + 10e^{\left(-\frac{6J}{kT}\right)} + 14e^{\left(\frac{6J}{kT}\right)} + 12e^{\left(-\frac{7J}{kT}\right)} + 16e^{\left(\frac{7J}{kT}\right)} + 14e^{\left(-\frac{8J}{kT}\right)}
 \end{aligned}$$

A nonlinear least-squares fit between 300-1.8 K leads to a value of $J = 0.22 \text{ cm}^{-1}$, $g=2.0$ ($R=8 \times 10^{-6}$, $R=\frac{\sum(\chi_m T_{\text{obs}}) - (\chi_m T_{\text{exp}})^2}{\sum(\chi_m T_{\text{obs}})^2}$). For **1** and **2** the positive J value corroborates the ferromagnetic nature of the interaction between the Cu^{II} - Gd^{III} spin carriers as has been reported for analogous systems,^{16,83,84} however the quality of the fit are different. In **1**, the dinuclear model cannot reproduce the experimental data in the low temperature range, due to the $\chi_m T$ value at 1.8 K ($13.06 \text{ emu K mol}^{-1}$) is higher than the expected for a ferromagnetic coupled Cu-Gd isolated binuclear system ($10 \text{ emu K mol}^{-1}$). This fact indicates that a higher magnetic dimensionality should be consider for **1**, i.e. a genuine 1D magnetic network is observed. Meanwhile in **2**, the experimental data are well reproduced in the whole temperature range by the use the trinuclear Gd-Cu-Gd model, indicating that in the case of **2** the Gd-Gd interactions

1
2
3 are small enough to be hidden by the stronger Gd-Cu-Gd interactions, thus behaving as isolated
4
5
6 trinuclear cores in the crystal lattice.
7

8
9 Spin polarization has been postulated by Gatteschi et al. to explain this magnetic interaction
10
11 between Cu^{II}-Gd^{III} cations.^{85,86} This mechanism is based on the partial delocalization of the *3d*
12
13 unpaired electron of the Cu^{II} toward the empty *6s* or *5d* orbitals of Gd^{III} with the same spin of the
14
15 seven *f* electrons, in order to obey Hund's rule. Thus, a ferromagnetic pathway can be
16
17 established when a magnetic orbital of one paramagnetic site has a non-zero overlap with an
18
19 empty orbital of the other site.⁸⁷ Most of the studied Cu^{II}-Gd^{III} systems are 0D complexes formed
20
21 by dioxo bridges (alcoxo or phenoxo). The magneto-structural correlations show that planar
22
23 conformation in Cu-dioxo-Gd moieties and shorter Cu...Gd distances lead to stronger
24
25 ferromagnetic interactions.⁸⁸ On the other hand, carboxylate bridges have been less studied
26
27 since this group mediates weaker magnetic interactions than the oxo bridge due to the longer
28
29 Cu...Gd distances; as far as we know no systematic studies have been made up to date.
30
31 Regarding the different types of carboxylate bridges, the *syn-anti* conformation has been
32
33 reported to mediate poor⁸⁹ or null magnetic interaction between Cu^{II} and Gd^{III},^{90,91} while the *anti-*
34
35 *anti* conformation produces weak ferromagnetic interactions.^{16,36} For example, Liu et al reported
36
37
38
39
40
41
42
43
44
45
46
47
48
49
50
51
52
53
54
55
56
57
58
59
60

1
2
3 a 3D HCP $\{[\text{GdCu}(\text{L}^1)_2(\text{L}^2)(\text{H}_2\text{O})_2] \cdot m\text{H}_2\text{O}\}_n$ (H_2L^1 = quinolinic acid, HL^2 = nicotinic acid), in which
4
5
6 the *anti-anti* carboxylate bridges of quinolinate and nicotinate ligands generate a $\text{Cu} \cdots \text{Gd}$
7
8
9 distance of 6.010 Å, with a ferromagnetic coupling of $J = 0.426 \text{ cm}^{-1}$.⁹² On the other hand, Zou
10
11
12 et al. found a slightly stronger magnetic interaction of $J = 1.30(3) \text{ cm}^{-1}$ between $\text{Cu}^{\text{II}}-\text{Gd}^{\text{III}}$ for a
13
14
15 shorter inter-cation distance of 5.991 Å in the 1D compound $[\text{Gd}(\text{H}_2\text{O})_3(\text{NO}_3)(\text{CuL})_2] \cdot \text{H}_2\text{O}$ ($\text{H}_3\text{L} =$
16
17
18
19
20
21
22
23
24
25
26
27
28
29
30
31
32
33
34
35
36
37
38
39
40
41
42
43
44
45
46
47
48
49
50
51
52
53
54
55
56
57
58
59
60
glycylglycine-N-[1-(2-hydroxy, phenyl)-propylidene]).⁹³ These facts are in agreement with that
observed in **1** and **2**, in which the shorter $\text{Cu} \cdots \text{Gd} = 6.1378 \text{ Å}$ distance, present in **1**, produces a
slightly higher magnetic coupling ($J = 0.60 \text{ cm}^{-1}$) compared with the coupling constant in **2**, ($J =$
 0.22 cm^{-1} for a $\text{Cu} \cdots \text{Gd} = 6.226 \text{ Å}$). Hence, beyond of the structural complexity that present **1** and
2 networks, the simplification of the structures leads to some interesting magneto-structural
correlations.

4. CONCLUDING REMARKS

Despite the difficulty to include at the same time Cu^{I} and Cu^{II} in an *3d-4f* heterometallic
extended network, two novel $\text{Cu}^{\text{I}}/\text{Cu}^{\text{II}}-\text{Gd}^{\text{III}}$ HCP $[\text{Gd}(\text{H}_2\text{O})_4\text{Cu}^{\text{II}}\text{Cu}^{\text{I}}(\text{IDC})_2]$ **1** and
 $[\text{Gd}_2(\text{H}_2\text{O})_2(\text{C}_2\text{O}_4)_2\text{Cu}^{\text{II}}(\text{IDC})_2\text{Cu}^{\text{I}}_2(4,4'\text{-bipy})] \cdot 4.5\text{H}_2\text{O}$ **2** have been successfully synthesized by
solvothermal synthesis, using 1H-imidazole-4,5-dicarboxylic acid (H_3IDC) as principal N,O-

1
2
3 bifunctional organic linker. Both **1** and **2** was obtained by the partial reduction of Cu^{II} under
4
5
6 autogenerated pressure, being the stabilization of Cu^I achieved only thanks to the coordination
7
8
9 of N-donor ligands. Interestingly, in the case of **1**, the simplicity of the chemical composition it is
10
11
12 highlighted offering a path of synthesis where only one ligand is necessary to coordinate and
13
14
15 stabilize three different cations. The proposed modification of the synthesis of **1** result
16
17
18 successfully in the obtention of a second new mixed valence *3d-4f* HCP **2**, with a superior
19
20
21 structural complexity. Compound **1** presents a honeycomb topology 2D network in which the
22
23
24 crystal packing is achieved by hydrogen bonding between coordinated water molecules and the
25
26
27 carboxylate groups. Meanwhile, in the case of **2** the addition of the extra organic linker permits
28
29
30
31 to obtain a 3D structure.
32
33
34
35

36
37
38 From a magnetic point of view, **1** and **2** behave as paramagnets at high temperature, showing
39
40
41 ferromagnetic interactions from 50 K to 1.8 K. It is important to point out that the use of simple
42
43
44 analytical models was useful to determine which interactions are predominant, thus extracting
45
46
47 the magnetic coupling constant for the principal exchange interaction between the *3d-4f* spin
48
49
50 carriers. Remarkably, the inclusion of Cu^I/Cu^{II} mixed valence cations in a *3d-4f* coordination
51
52
53
54
55 polymers offers a potential strategy to the rational design of new metal-organic materials, where
56
57
58
59
60

the individual properties of the lanthanide cations can be used to the generation of new multifunctional materials.

TABLES

Table 1. Crystal data and structure refinement for **1** and **2**

Table 2. Table 2 Hydrogen Bonds for **1**

Table 1 Crystal data and structure refinement for **1** and **2**

Compound code	1	2
Compound formula	[Gd(H ₂ O) ₄ Cu ^{II} Cu ^I (IDC) ₂]	[Gd ₂ (H ₂ O) ₂ (C ₂ O ₄) ₂ Cu ^{II} (IDC) ₂ Cu ^I ₂ (4,4'-bipy)]·4.5H ₂ O
Empirical formula	C ₁₀ H ₁₀ Cu ₂ GdN ₄ O ₁₂	Cu _{1.5} GdC ₁₂ H _{11.5} N ₃ O _{11.25}
Formula weight	662.53	630.34
Temperature/K	150	150
Crystal system	Triclinic	Triclinic
Space group	<i>P</i> $\bar{1}$	<i>P</i> $\bar{1}$
<i>a</i> /Å	6.6701(5)	8.5247(7)
<i>b</i> /Å	11.3064(9)	9.6931(9)
<i>c</i> /Å	12.0027(11)	12.0429(11)
α /°	62.710(3)	102.413(3)

$\beta/^\circ$	82.646(3)	102.608(3)
$\gamma/^\circ$	78.035(3)	111.608(3)
Volume/ \AA^3	786.39(11)	853.70(13)
Z	2	2
$\rho_{\text{cal}}/\text{g/cm}^3$	2.790	2.407
μ/mm^{-1}	6.930	5.769
F(000)	628.0	585.0
Crystal size/ mm^3	0.15 × 0.03 × 0.025	0.08 × 0.05 × 0.04
Radiation	MoK α ($\lambda = 0.71073$)	MoK α ($\lambda = 0.71073$)
2 θ range for data collection/ $^\circ$	4.112 to 55.024	4.78 to 55.064
Reflections collected	3614	19557
Independent reflections	3614 [Rint = 0.0191, Rsigma = 0.0307]	3923 [Rint = 0.0214, Rsigma = 0.0170]
Data/restraints/parameters	3614/18/281	3923/18/278
Goodness-of-fit on F ²	1.096	1.131
Final R indexes [$I \geq 2\sigma(I)$]	R1 = 0.0192, wR2 = 0.0453	R1 = 0.0232, wR2 = 0.0619
Final R indexes [all data]	R1 = 0.0234, wR2 = 0.0464	R1 = 0.0251, wR2 = 0.0632

1
2
3 Largest diff. 1.03/-0.83 1.39/-1.40
4 peak/hole / e Å⁻³
5
6
7
8
9
10

11
12 Table 2 Hydrogen Bonds for 1
13

D	H	A	d(D-H)/Å	d(H-A)/Å	d(D-A)/Å	D-H-A/°
O1W	H1WA	O51	0.825(9)	1.916(15)	2.721(3)	165(4)
O1W	H1WB	O42	0.827(9)	1.931(11)	2.756(3)	176(5)
O2W	H2WB	O43	0.89	1.85	2.683(3)	155.4
O3W	H3WB	O14	0.90	1.96	2.840(3)	165.0

24
25
26
27
28
29 FIGURE CAPTIONS
30

31
32 Figure 1. Scheme of synthesis of 1 and 2.
33
34
35

36
37 Figure 2. Coordination modes of (a) IDC³⁻, (b) 4,4'-bipyridine and C₂O₄²⁻ in 1 and 2.
38
39

40
41 Figure 3. Coordination environment of (a) Cu1, (b) Cu2 and (c) Gd1 cations present in 1.
42
43
44

45
46 Figure 4. (a) Hexagonal honeycomb 2D extended structure, (b) simplified structure of 1, (c)
47
48 scheme for the [Gd(H₂O)₄]³⁺ tripod moiety inserted in a hexagonal cavity and (d) supramolecular
49
50
51
52
53 packing of 1 layers through H-bond.
54
55
56
57
58
59
60

1
2
3 Figure 5. Coordination environment of (a) Cu1, (b) Cu2 and (c) Gd1 in **2**.
4
5
6

7 Figure 6. View of the assembly of the extended structure of **2** through a axis, (a) in pink, Gd^{III}-
8 oxalate based chains, in green, Cu^I/Cu^{II} mixed valence chains and (b) scheme of the connection
9
10
11
12
13
14 between Gd^{III}-oxalate and Cu^I/Cu^{II} through IDC³⁻ linking.
15
16
17

18 Figure 7. Thermogram between 25° and 900°C under N₂ atmosphere for **1** and **2** (inset) and in
19
20
21
22
23
24
25
26
27
28
29
30
31
32
33
34
35
36
37
38
39
40
41
42
43
44
45
46
47
48
49
50
51
52
53
54
55
56
57
58
59
60
in situ temperature-dependent X-ray diffraction (TDXD) under N₂ atmosphere was performed for
1.

Figure 8. $\chi_m T$ vs T plot at 1 kOe between 300 and 1.8 K for **1** and **2**. In the inset, scheme of the
Cu^{II}-Gd^{III} and Cu^{II}-Gd^{III}-Cu^{II} moieties used in **1** and **2** for magnetic data analysis.

Figure 9. Isothermal magnetization represented by reduced magnetization (N_β) at 1.8, 3, 5 and
8 K between 0-90 kOe for (a) **1** and (b) **2**.

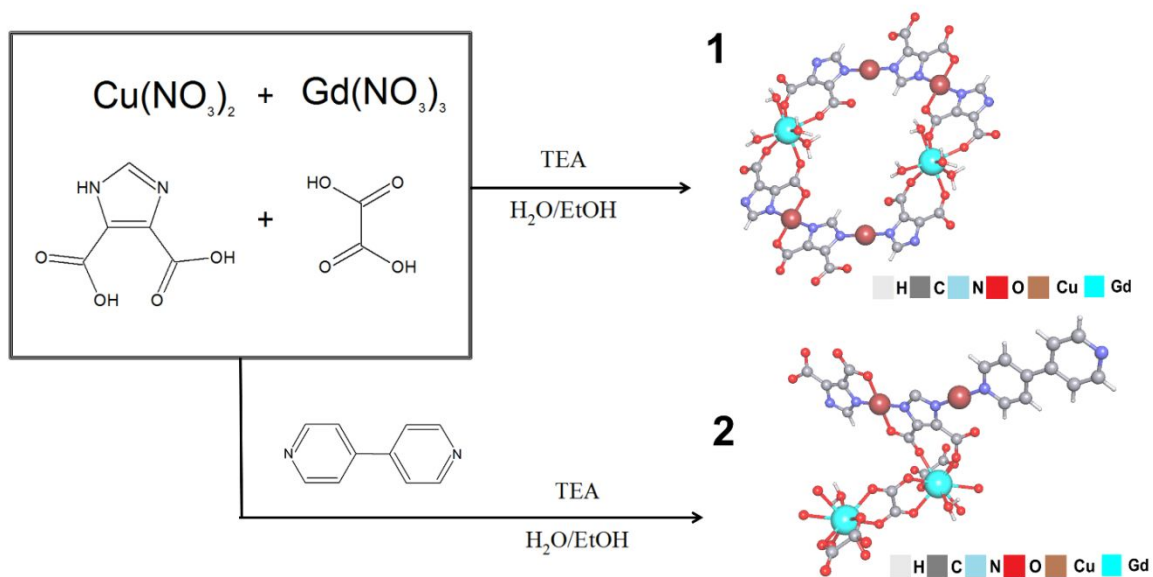


Figure 1

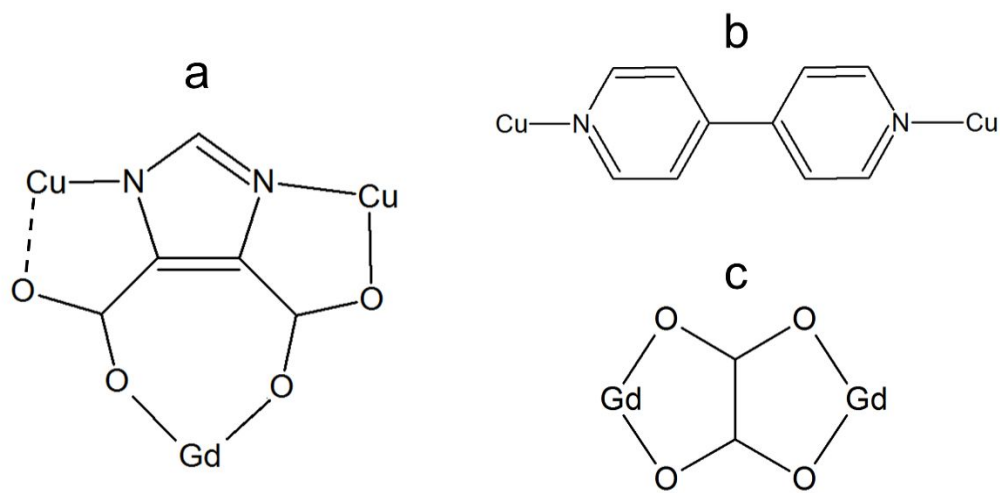


Figure 2

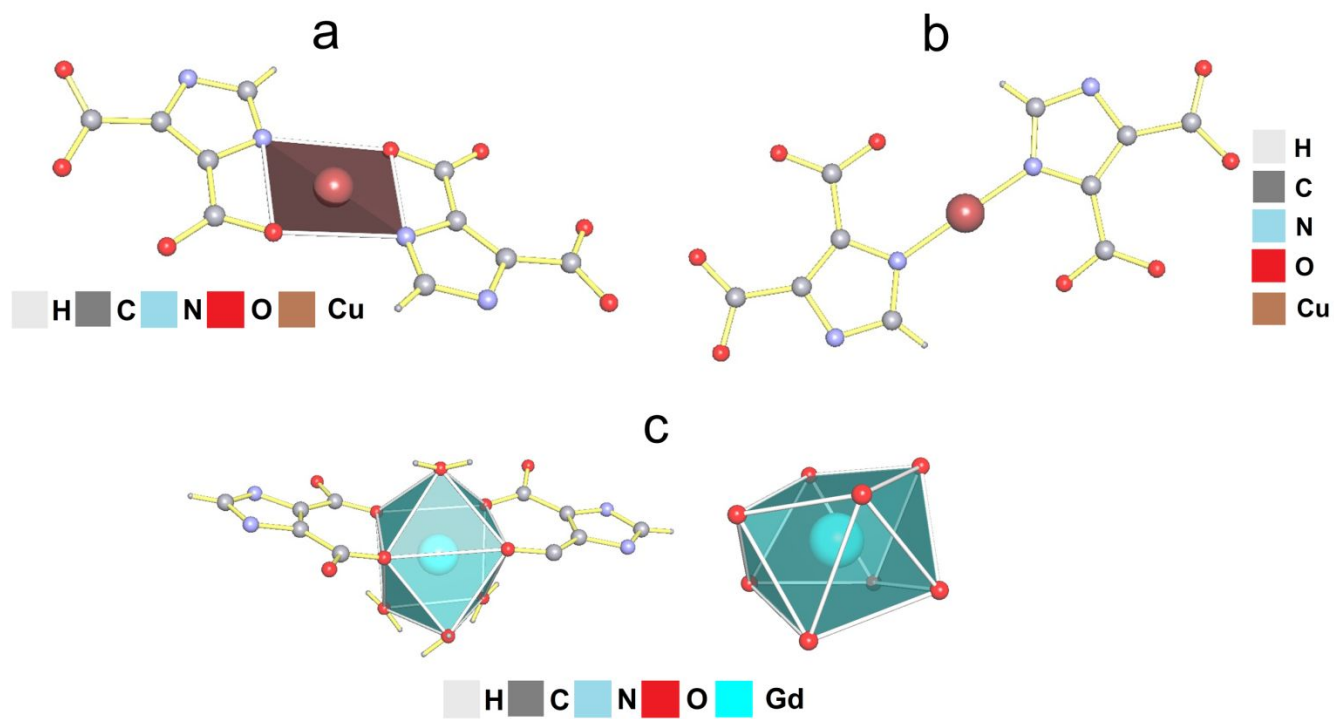


Figure 3

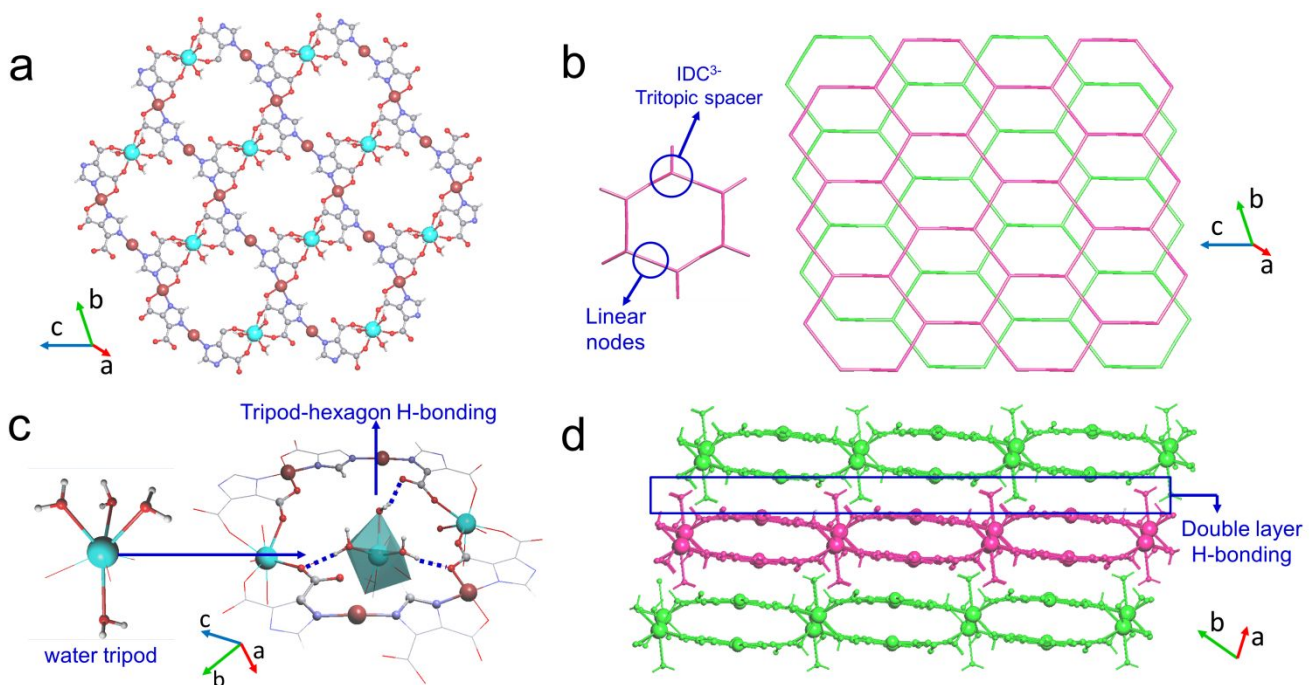


Figure 4

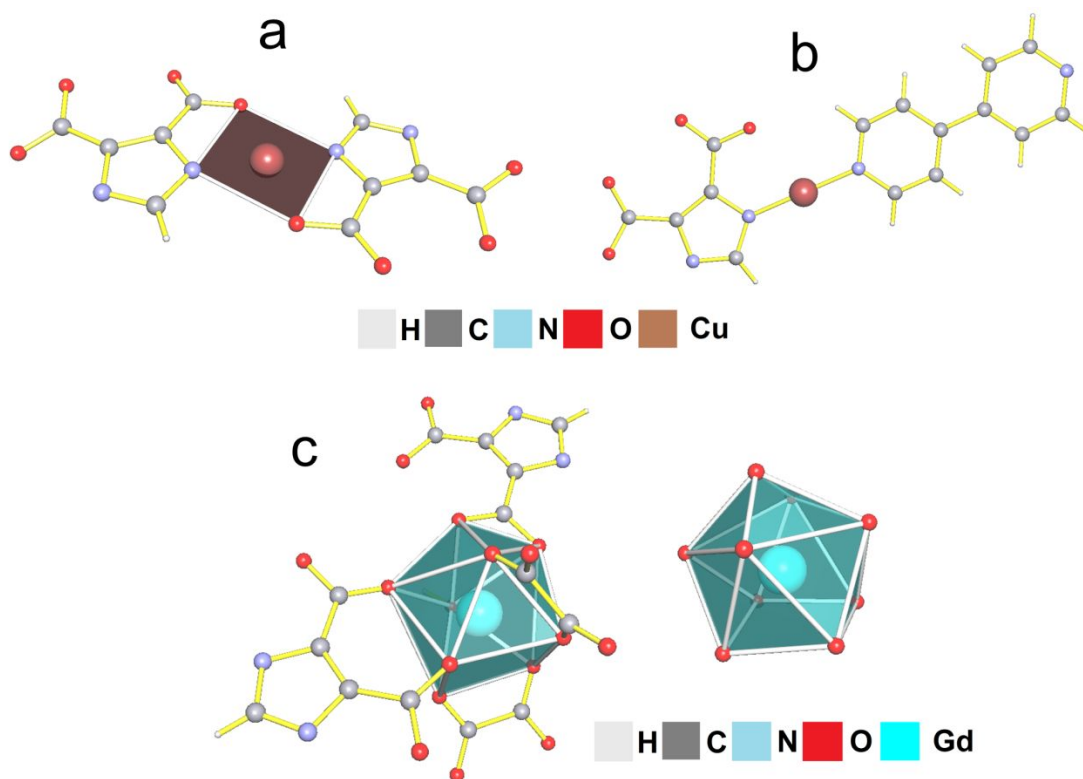


Figure 5

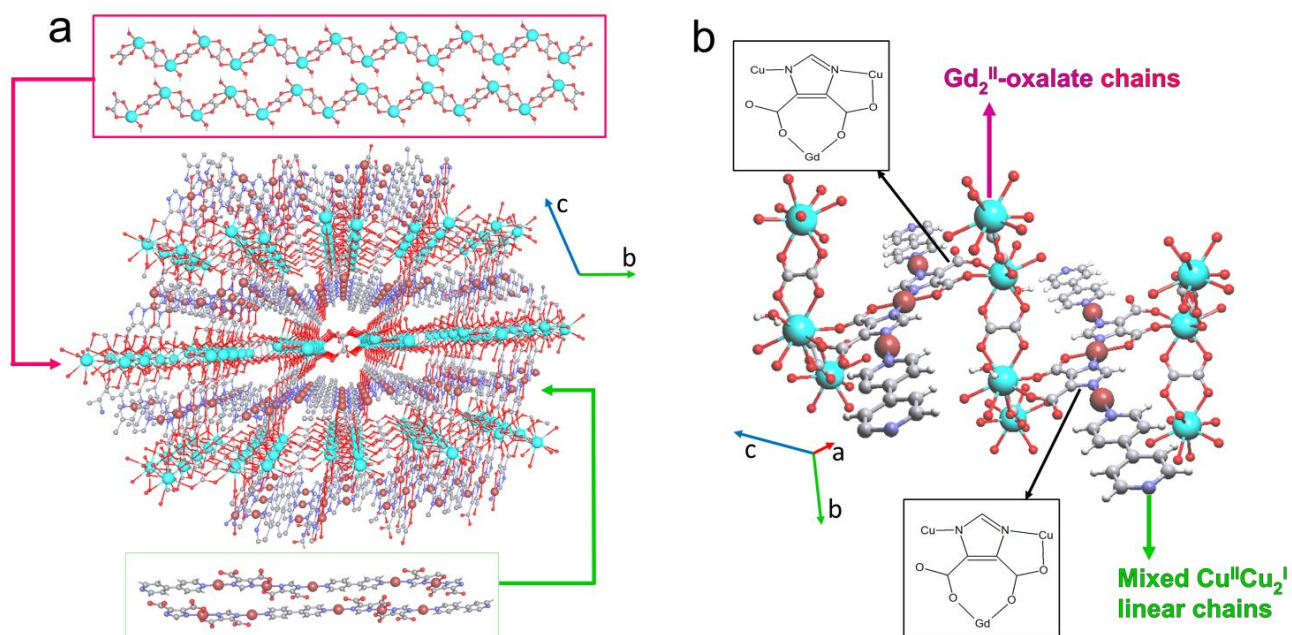


Figure 6

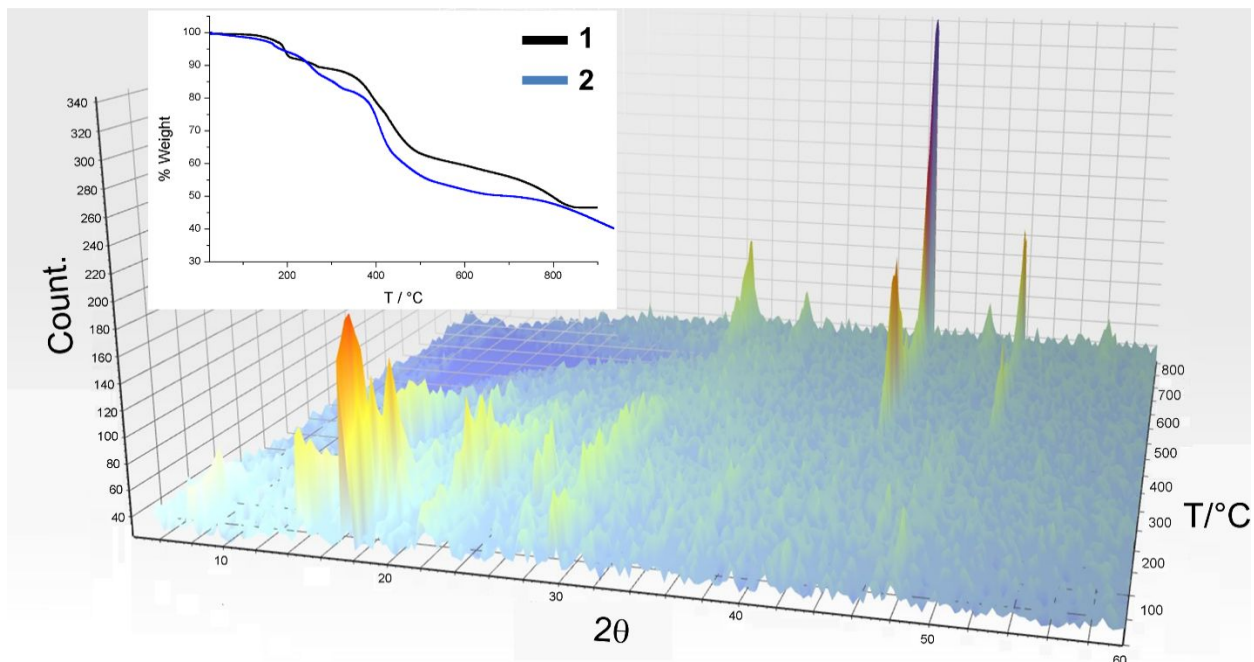


Figure 7

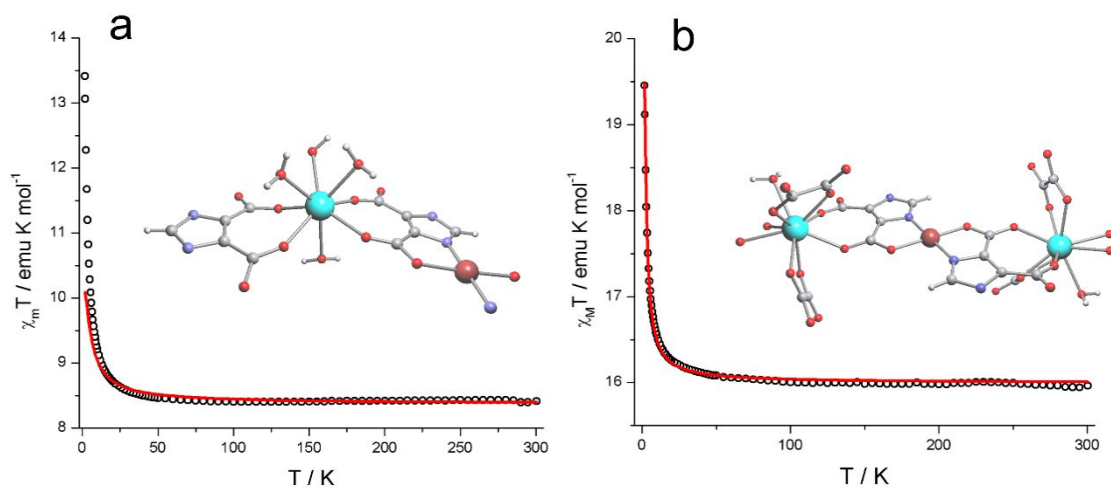


Figure 8

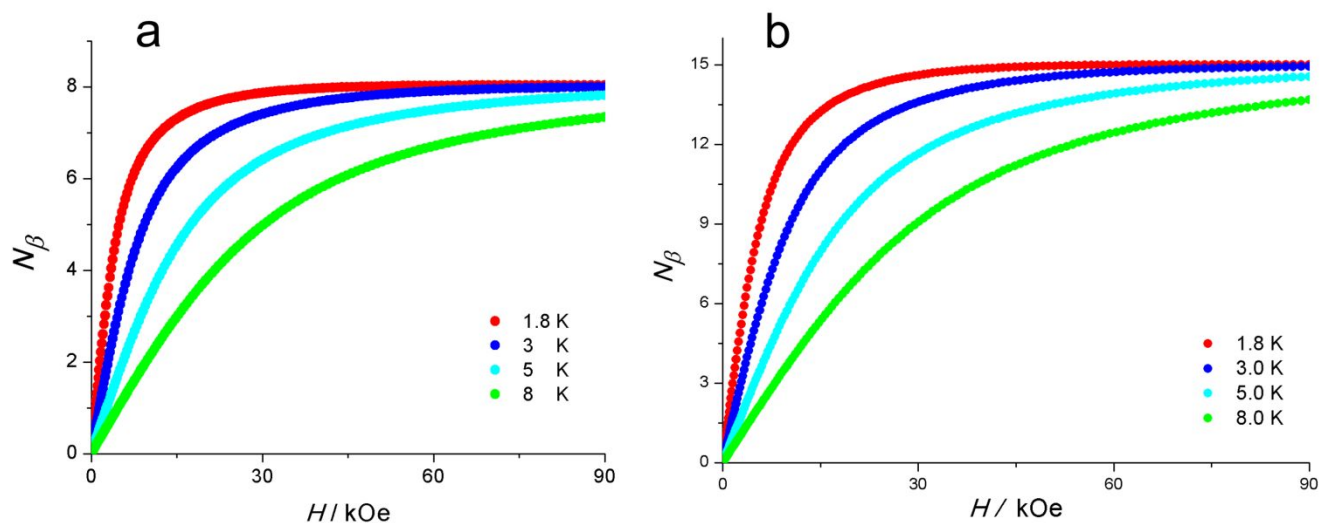


Figure 9

ASSOCIATED CONTENT

Supporting Information.

The following files are available free of charge, experimental and calculated Powder X-Ray diffraction pattern of **1** (Figure S1), UV-Vis spectra for **1** and **2** (Figure S2) and complete crystallographic refinement data for **1** and **2** (Table S1 and S2)

Accession Codes CCDC 1915837-1915838 contains the supplementary crystallographic data for this publication. These data can be obtained free of charge via www.ccdc.cam.ac.uk/data_request/cif, or by emailing data_request@ccdc.cam.ac.uk, or by

1
2
3 contacting The Cambridge Crystallographic Data Centre, 12 Union Road, Cambridge CB2 1EZ,
4
5
6 UK; fax: +44 1223 336033.
7
8
9

10 AUTHOR INFORMATION
11
12
13

14
15 Corresponding Author
16
17
18

19 *V.P-G.: e-mail, vparedes@unab.cl; tel, +56-2-2661 5756.
20
21
22

23 Acknowledgements: The authors acknowledge FONDECYT 1170887, Proyecto Anillo
24
25

26
27 CONICYT ACT 1404 grant, CONICYT-FONDEQUIP/PPMS/EQM130086-UNAB, Chilean-
28
29

30 French International Associated Laboratory for Multifunctional Molecules and Materials-LIAM3-
31
32

33
34 CNRS N°1027 and ECOS/CONICYT C15E02. Authors acknowledge CEDENNA,
35
36

37 Financiamiento Basal, FB0807. The authors also acknowledge the support of the Laboratory of
38
39

40
41 Analyses of Solids (L.A.S-UNAB). REFERENCES
42
43
44

45 (1) Liu, H.; Kang, Y. an; Fan, Y. P.; Guo, F. S.; Liu, L.; Li, J. L.; Liu, P.; Wang, Y. Y. High
46
47

48 Thermally and Chemically Stable Nickel(II) Coordination Polymers: Tentative Studies on
49
50

51
52 Their Sorption, Catalysis, and Magnetism. *Cryst. Growth Des.* **2018**, *19*, 797–807.
53
54
55
56
57
58
59
60

- 1
2
3 (2) Hao, X. M.; Qu, T. G.; Wang, H.; Guo, W. L.; Chen, F.; Wu, Y. B.; Yang, D.; Xu, Z. L. A
4
5
6 3D Porous Coordination Polymer Transformed from a 1D Nonporous Coordination
7
8
9
10 Polymer for Selectively Sensing of Diiodomethane. *J. Solid State Chem.* **2018**, *268*, 62–
11
12
13 66.
14
15
16
17 (3) Li, Y. M.; Li, X. F.; Wu, Y. Y.; Collins Wildman, D.; Hu, S. M.; Liu, Y.; Li, H. Y.; Zhao, X.
18
19
20
21 W.; Jin, L. Y.; Dang, D. Bin. Ni^{II}, Mn^{II}, and Co^{II} Coordination Polymers with 1,4-
22
23
24 Naphthalenedicarboxylic Acid Exhibiting Metamagnetic and Antiferromagnetic
25
26
27
28 Behaviors. *Cryst. Growth Des.* **2018**, *18*, 7541–7547.
29
30
31
32 (4) Wang, P.; Fan, R. Q.; Yang, Y. L.; Liu, X. R.; Xiao, P.; Li, X. Y.; Hasi, W.; Cao, W. W. 1-
33
34
35
36 D Helical Chain, 2-D Layered Network and 3-D Porous Lanthanide-Organic Frameworks
37
38
39 Based on Multiple Coordination Sites of Benzimidazole-5,6-Dicarboxylic Acid: Synthesis,
40
41
42
43 Crystal Structure, Photoluminescence and Thermal Stability. *CrystEngComm* **2013**, *15*,
44
45
46 4489–4506.
47
48
49
50 (5) Bing, Y.; Xu, N.; Shi, W.; Liu, K.; Cheng, P. Two Lanthanide(III)-Copper(II) Organic
51
52
53
54 Frameworks Based on {OLn₆} Clusters That Exhibited a Large Magnetocaloric Effect
55
56
57
58
59
60

1
2
3 and Slow Relaxation of the Magnetization. *Chem. Asian J.* **2013**, *8*, 1412–1418.

- 4
5
6
7 (6) Dong, R. T.; Chen, X. L.; Cui, X.; Chen, S. S.; Shen, M. Y.; Li, C. W.; Li, Q. H.; Hu, M.
8
9
10 Y.; Huang, L. F.; Deng, H. Copper(I)-Lanthanide(III) Heterometallic Metal-Organic
11
12 Frameworks Constructed from 3-(3-Pyridyl)Acrylic Acid: Syntheses, Structures, and
13
14 Properties. *CrystEngComm* **2016**, *18*, 5547–5561.
15
16
17
18
19
20
21 (7) Li, X.; Huang, Y.; Cao, R. Three-Dimensional Pillared-Layer 3d-4f Heterometallic
22
23
24 Coordination Polymers with or without Halides. *Cryst. Growth Des.* **2012**, *12*, 3549–
25
26
27
28
29 3556.
30
31
32
33 (8) He, X.; Liu, Y.; Lv, Y.; Dong, Y.; Hu, G.; Zhou, S.; Xu, Y. L- And D-[LnZn(IN)₃(C₂H₄O₂)_n]
34
35
36 (Ln = Eu, Sm, and Gd): Chiral Enantiomerically 3D 3d-4f Coordination Polymers
37
38
39 Constructed by Interesting Butterfly-like Building Units and -[Ln-O-Zn]_n- Helices. *Inorg.*
40
41
42
43
44
45
46
47
48 (9) Yang, T. H.; Silva, A. R.; Shi, F. N. Six New 3d-4f Heterometallic Coordination Polymers
49
50
51 Constructed from Pyrazole-Bridged Cu(II)Ln(III) Dinuclear Units. *Dalt. Trans.* **2013**, *42*,
52
53
54
55 13997–14005.
56
57
58
59
60

- 1
2
3 (10) Yang, T. H.; Silva, A. R.; Fu, L.; Shi, F. N. Synthesis, Crystal Structure, and Catalytic
4
5
6 Properties of Porous 3d-4f Heterometallic Coordination Polymers Constructed from
7
8
9 Pyrazine-2,3-Dicarboxylic Acid. *Zeitschrift für Anorg. und Allg. Chemie* **2017**, *643*, 1801–
10
11
12 1808.
13
14
15
16
17 (11) Shaowei, Z.; Peng, C. Recent Advances in the Construction of Lanthanide-Copper
18
19
20 Heterometallic Metal-Organic Frameworks. *CrystEngComm* **2015**, *17*, 4250–4271.
21
22
23
24
25 (12) Fedin, M. V.; Veber, S. L.; Bagryanskaya, E. G.; Ovcharenko, V. I. Electron
26
27
28 Paramagnetic Resonance of Switchable Copper-Nitroxide-Based Molecular Magnets: An
29
30
31 Indispensable Tool for Intriguing Systems. *Coord. Chem. Rev.* **2015**, *289–290*, 341–356.
32
33
34
35
36 (13) Rentschler, E.; Gatteschi, D.; Cornia, A.; Fabretti, A. C.; Barra, A.L.; Shchegolikhina, O.
37
38
39 I.; Zhdanov, A. A. Molecule-Based Magnets: Ferro- and Antiferromagnetic Interactions in
40
41
42 Copper (II)-Polyorganosiloxanolate Clusters. *Inorg. Chem.* **1996**, *1669*, 4427–4431.
43
44
45
46
47 (14) Bencini, A.; Benelli, C.; Caneschi, A.; Carlin, R. L.; Dei, A.; Gatteschi, D. Crystal and
48
49
50 Molecular Structure of and Magnetic Coupling in Two Complexes Containing
51
52
53 Gadolinium(III) and Copper(II) Ions. *J. Am. Chem. Soc.* **1985**, *107*, 8128–8136.
54
55
56
57
58
59
60

- 1
2
3 (15) Andruh, M.; Costes, J. P.; Diaz, C.; Gao, S. 3d-4f Combined Chemistry: Synthetic
4
5
6 Strategies and Magnetic Properties. *Inorg. Chem.* **2009**, *48*, 3342–3359.
7
8
9
- 10 (16) Manna, S. C.; Konar, S.; Zangrando, E.; Ribas, J.; Ray Chaudhuri, N. 3D Heterometallic
11
12
13 (3d-4f) Coordination Polymers: A Ferromagnetic Interaction in a Gd(III)-Cu(II) Couple.
14
15
16
17 *Polyhedron* **2007**, *26*, 2507–2516.
18
19
20
- 21 (17) Li, Z. Y.; Wang, Y. X.; Zhu, J.; Liu, S. Q.; Xin, G.; Zhang, J. J.; Huang, H. Q.; Duan, C. Y.
22
23
24
25 Three Series of 3d-4f Heterometallic Polymers Based on [LnCu₆] or [Ln₆Cu₂₄] Clusters
26
27
28 and Formate Bridges: Displaying Significant Magnetocaloric Effect. *Cryst. Growth Des.*
29
30
31
32 **2013**, *13*, 3429–3437.
33
34
35
- 36 (18) Pavlishchuk, A. V; Kolotilov, S. V; Zeller, M.; Thompson, L. K.; Addison, A. W. Formation
37
38
39 of Coordination Polymers or Discrete Adducts via Reactions of
40
41
42
43 Gadolinium(III)–Copper(II) 15-Metallacrown-5 Complexes with Polycarboxylates:
44
45
46
47 Synthesis, Structures and Magnetic Properties. *Inorg. Chem.* **2014**, *53*, 1320–1330.
48
49
50
- 51 (19) Yang, T. H.; Silva, A. R.; Shi, F. N. Six New 3d-4f Heterometallic Coordination Polymers
52
53
54
55 Constructed from Pyrazole-Bridged Cu^{II}Ln^{III} dinuclear Units. *Dalt. Trans.* **2013**, *42*,
56
57
58
59
60

1
2
3 13997–14005.
4
5
6

7 (20) Xin, N.; Sun, Y. Q.; Zheng, Y. F.; Xu, Y. Y.; Gao, D. Z.; Zhang, G. Y. Seven 3d-4f
8

9
10 Coordination Polymers of Macrocyclic Oxamide with Polycarboxylates: Syntheses,
11

12
13
14 Crystal Structures and Magnetic Properties. *J. Solid State Chem.* **2016**, *243*, 267–27.
15

16
17
18 (21) Zeng, G.; Xing, S.; Wang, X.; Yang, Y.; Ma, D.; Liang, H.; Gao, L.; Hua, J.; Li, G.; Shi,
19

20
21 Z.; Feng S. 3d-4f Metal-Organic Framework with Dual Luminescent Centers That
22

23
24
25 Efficiently Discriminates the Isomer and Homologues of Small Organic Molecules. *Inorg.*
26

27
28
29 *Chem.* **2016**, *55*, 1089–1095.
30

31
32
33 (22) Xu, H.; Cao, C. S.; Xue, J. Z.; Xu, Y.; Zhai, B.; Zhao, B. A Cuprous/Lanthanide-Organic
34

35
36 Framework as the Luminescent Sensor of Hypochlorite. *Chem. - A Eur. J.* **2018**, *24*,
37

38
39
40 10296–10299.
41

42
43
44 (23) Wu, A. Q.; Guo, G. H.; Yang, C.; Zheng, F. K.; Liu, X.; Guo, G. C.; Huang, J. S.; Dong,
45

46
47 Z. C.; Takano, Y. Extended Structures and Magnetic Properties of Lanthanide-Copper
48

49
50
51 Complexes with Picolinic Acids as Bridging Ligands. *Eur. J. Inorg. Chem.* **2005**, *10*,
52

53
54
55 1947–1954.
56
57
58
59
60

- 1
2
3 (24) Bo, Q. B.; Sun, Z. X.; Forsling, W. A New Family of 3D 3d-4f Heterometallic Frameworks
4
5
6 Comprising 1D Inorganic Lanthanide Ladders and Organic Cu^I-Bipyridine Chains.
7
8
9
10 *CrystEngComm* **2008**, *10*, 232–238.
11
12
13
14 (25) Bo, Q. B.; Sun, G. X.; Geng, D. L. Novel Three-Dimensional Pillared-Layer Ln(III)-Cu(I)
15
16
17 Coordination Polymers Featuring Spindle-Shaped Heterometallic Building Units. *Inorg.*
18
19
20
21 *Chem.* **2010**, *49*, 561–571.
22
23
24
25 (26) Sun, Y. N.; Xiong, G.; Dragutan, V.; Dragutan, I.; Ding, F.; Sun, Y. G. Novel Luminescent
26
27
28 Heterobimetallic Ln-Cu(I) 3D Coordination Polymers Based on 5-(4-Pyridyl) Isophthalic
29
30
31
32 Acid as Heteroleptic Ligand. Synthesis and Structural Characterization. *Inorg. Chem.*
33
34
35
36 *Commun.* **2015**, *62*, 103–106.
37
38
39
40 (27) Ay, B.; Karaca, S.; Yildiz, E.; Lopez, V.; Nanao, M. H.; Zubieta, J. In Situ Hydrothermal
41
42
43
44 Syntheses, Structures and Photoluminescent Properties of Four Novel Metal-Organic
45
46
47 Frameworks Constructed by Lanthanide (Ln=Ce(III), Pr(III), Eu(III)) and Cu(I) Metals with
48
49
50 Flexible Dicarboxylate Acids and Piperazine-Based Ligands. *J. Solid State Chem.* **2016**,
51
52
53
54 *233*, 415–421.
55
56
57
58
59
60

- 1
2
3 (28) Zhu, Z. B.; Zeng, H. P. A 3-D Gd(III)–Cu(I) Coordination Polymer Based on Nicotinate
4
5
6 and Oxalate Ligands: Synthesis, Crystal Structure, and Magnetic Properties. *J. Coord.*
7
8
9
10 *Chem.* **2010**, *63*, 2097–2104.
- 11
12
13
14 (29) Wu, S. A Novel Three-Dimensional Hetero-Metallic Coordination Polymer: Poly[[diaqua-
15
16
17 di- μ_3 -chlorido- μ_2 -chlorido-tri- μ_3 -nicotinato-tricopper(I)gadolinium(III)] hemihydrate]. *Acta*
18
19
20
21 *Crystallogr. Sect. C Cryst. Struct. Commun.* **2011**, *C67*, 211–214.
- 22
23
24
25 (30) Cao, G. J.; Li, Q. L.; Rong, C.; Wang, Y. L. A Tubular One-Dimensional Polymer
26
27
28
29 Constructed from Alternating Clusters of Europium(III)-Water and Copper(I) Chloride
30
31
32 Bridged by 4-(Pyridin-4-yl)Benzoate. *Acta Crystallogr. Sect. C Cryst. Struct. Commun.*
33
34
35
36 **2013**, *C69*, 712–715.
- 37
38
39
40 (31) Fang, W. H.; Yang, G. Y. Three Pillared-Layer 3d-4f Heterometallic Frameworks Based
41
42
43
44 on Tetranuclear Lanthanide Clusters. *CrystEngComm* **2013**, *15*, 4504–4512.
- 45
46
47
48 (32) Xia, C.; Xiong, G.; You, L.; Ren, B.; Wang, S.; Sun, Y. Synthesis, Crystal Structure, and
49
50
51
52 Photoluminescent Properties of a Series of Ln^{III}-Cu^I Heterometallic Coordination
53
54
55
56 Polymers Based on Cu₄I₃ Clusters and Ln-Ina Rod Units. *Aust. J. Chem.* **2017**, *70*, 943–
57
58
59
60

1
2
3 951.
4
5
6

7 (33) Fang, W. H.; Cheng, J. W.; Yang, G. Y. Two Series of Sandwich Frameworks Based on
8
9
10 Two Different Kinds of Nanosized Lanthanide(III) and Copper(I) Wheel Cluster Units.
11
12
13
14 *Chem. - A Eur. J.* **2014**, *20*, 2704–2711.
15
16

17
18 (34) Chen, H. M.; Hu, R. X.; Zhang, M. B. Heterometallic Coordination Polymers Constructed
19
20
21 by Linear Ligands. *Inorganica Chim. Acta* **2011**, *379*, 34–39.
22
23
24
25

26 (35) Luo, F.; Che, Y. X.; Zheng, J. M. The First Self-Penetrating Topology Based on an
27
28
29 Unusual α -Po Net with Double Edges Constructed from a 12-Connected $Gd_2(\mu_2-$
30
31
32 $O_{\text{carboxylate}})_2(\mu_2-OH)_2(\mu_3-OH)_2Cu_2$ Core. *Cryst. Growth Des.* **2006**, *6*, 2432–2434.
33
34
35
36

37 (36) Cruz, C.; Spodine, E.; Venegas-Yazigi, D.; Paredes-García, V. Cu(II)–Gd(III) 2D-
38
39
40 Coordination Polymer Based on Two Different Organic Linkers. *Polyhedron* **2017**, *136*,
41
42
43
44 117–124.
45
46
47

48 (37) Cruz, C.; Spodine, E.; Vega, A.; Venegas-Yazigi, D.; Paredes Garcia, V. Novel 3d/4f
49
50
51 Metal Organic Networks Containing Co(II) Chiral Chains. *Cryst. Growth Des.* **2016**, *16*
52
53
54
55 (4), 2173–2182.
56
57
58
59
60

- 1
2
3 (38) Cruz, C.; Spodine, E.; Audebrand, N.; Venegas-Yazigi, D.; Paredes-García, V. Structural
4
5
6 Versatility of 3d-Ce^{III} Heterometallic Coordination Polymers Using Co^{II} or Cu^{II}. *Cryst.*
7
8
9
10 *Growth Des.* **2018**, *18*, 5155–5165.
11
12
13
14 (39) APEX3 V2016.1-0. APEX3 V2016.1-0, Bruker AXS Inc.: Wisconsin, USA 2016.
15
16
17
18 (40) SAINT V6.22. SAINT V6.22 Bruker AXS Inc.: Madison, WI, USA 2000.
19
20
21
22
23 (41) SADABS V2.05. SADABS V2.05 Bruker AXS Inc.: Madison, WI, USA 2001.
24
25
26
27 (42) Dolomanov, O. V.; Bourhis, L. J.; Gildea, R. J.; Howard, J. A. K.; Puschmann, H.
28
29
30 OLEX2: A Complete Structure Solution, Refinement and Analysis Program. *J. Appl.*
31
32
33
34 *Crystallogr.* **2009**, *42*, 339–341.
35
36
37
38 (43) Sheldrick, G. M. SHELXT - Integrated Space-Group and Crystal-Structure
39
40
41
42 Determination. *Acta Crystallogr. Sect. A Found. Adv.* **2015**, *A71*, 3–8.
43
44
45
46 (44) Sheldrick, G. M. Crystal Structure Refinement with SHELXL. *Acta Crystallogr. Sect. C*
47
48
49
50 *Struct. Chem.* **2015**, *C71*, 3–8.
51
52
53
54 (45) Blatov, V.; Shevchenko, A. ToposPro, Program Package for Multipurpose
55
56
57
58
59
60

1
2
3 Crystallochemical Analysis. ToposPro V5.0, program package for multipurpose
4
5
6 crystallochemical analysis 2014.
7

8
9
10 (46) Bain, G. A.; Berry, J. F. Diamagnetic Corrections and Pascal's Constants. *J. Chem.*
11
12
13
14 *Educ.* **2008**, *85*, 532–536.
15

16
17
18 (47) Llunell, M.; Casanova, D.; Cirera, J.; Alemany, P.; Alvarez, S. SHAPE V2.1. SHAPE
19
20
21
22 V2.1, Departament de Química Física, Departament de Química Inorgànica, and Institut
23
24
25 de Química Teòrica i Computacional, Universitat de Barcelona: Barcelona, España
26
27
28
29 2013.
30

31
32
33 (48) Truong, Q. D.; Kakihana, M. Hydrothermal Growth of Cross-Linked Hyperbranched Copper
34
35
36 Dendrites Using Copper Oxalate Complex. *J. Cryst. Growth* **2012**, *348*, 65–70.
37

38
39 (49) Catalano, V. J.; Malwitz, M. A.; Etogo, A. O. Pyridine Substituted N-Heterocyclic
40
41
42 Carbene Ligands as Supports for Au(I)-Ag(I) Interactions: Formation of a Chiral
43
44
45 Coordination Polymer. *Inorg. Chem.* **2004**, *43*, 5714–5724.
46
47

48
49
50 (50) Irwin, M. J.; Vittal, J.; Yap, G. ; Puddephatt, R. Linear Gold (I) Coordination Polymers: A
51
52
53
54 Polymer with a Unique Sine Wave Conformation. *J. Am. Chem. Soc.* **1996**, *7863*,
55
56
57

1
2
3 13101–13102.
4
5
6

- 7 (51) Chen, C. L.; Kang, A. B. S.; Su, C. Y. Recent Advances in Supramolecular Design and
8
9
10
11 Assembly of Silver (I) Coordination Polymers. *Aust. J. Chem.* **2006**, *59*, 3–18.
12
13
14
15 (52) Tong, M. L.; Wu, Y. M.; Ru, J.; Chen, X. M.; Chang, H. C.; Kitagawa, S. Pseudo-
16
17
18 Polyrotaxane and β -Sheet Layer-Based Three-Dimensional Coordination Polymers
19
20
21
22 Constructed with Silver Salts and Flexible Pyridyl-Type Ligands. *Inorg. Chem.* **2002**, *41*,
23
24
25 4846–4848.
26
27
28
29 (53) Zhang, L. Y.; Lu, L. P.; Feng, S. S. A Two-Dimensional Mixed-Valence Cu^{II}/Cu^I
30
31
32
33 Coordination Polymer Constructed from 2-(Pyridin-3-yl)-1H-Imidazole-4,5-Dicarboxylate.
34
35
36
37 *Acta Crystallogr. Sect. C Struct. Chem.* **2016**, *C72*, 652–657.
38
39
40
41 (54) Visinescu, D.; Fabelo, O.; Ruiz-Pérez, C.; Lloret, F.; Julve, M, Synthesis, crystal
42
43
44 structure and magnetic properties of a new cyanide-bridged mixed-valence
45
46
47
48 copper(I)/copper(II) clathrate. *Inorg. Chem. Comm.* **2013**, *52*, 252-254.
49
50
51
52 (55) Fotouhi, L.; Dehghanpour, S.; Heravi, M.; Ardakani, M. Electrochemical Synthesis and
53
54
55
56 Structural Characterization of a Novel Mixed-Valence Copper (I)-Copper (II) Complex:
57
58
59
60

1
2
3 [[Bis(Ethylenediamine) Copper (II)] Bis[Diiodocuprate (I)]}. *Molecules* **2007**, *12*, 1410–
4
5
6 1419.

7
8
9
10 (56) De, S.; Chowdhury, S.; Naskar, J. P.; Drew, M. G. B.; Clérac, R.; Datta, D. A
11
12 Hexadecanuclear Copper(I)-Copper(II) Mixed-Valence Compound: Structure, Magnetic
13
14 Properties, Intervalence Charge Transfer, EPR, and NMR. *Eur. J. Inorg. Chem.* **2007**,
15
16 23, 3695–3700.

17
18
19
20 (57) Zhu, Y.; Wang, W.; Guo, M.; Li, G.; Lu, H. An Unprecedented 1-D Mixed-Valence
21
22 Cu(II)/Cu(I) Metal-Organic Framework Bearing 2-Phenyl Imidazole Dicarboxylates.
23
24 *Inorg. Chem. Acta* **2011**, *14*, 1432–1435.

25
26
27
28 (58) Day, P.; Hush, N.; Clark, R. Mixed Valence: Origins and Developments. *Philos. Trans.*
29
30 *R. Soc. A* **2008**, *366*, 5–14.

31
32
33
34 (59) Robin, M.; Day, P. Mixed Valence Chemistry-A Survey and Classification. *Adv. Inorg.*
35
36 *Chem. Radiochem.* **1967**, *10*, 247–422.

37
38
39
40 (60) Lu, W. G.; Jiang, L.; Feng, X. L.; Lu, T. B. Three 3D Coordination Polymers Constructed
41
42 by Cd(II) and Zn(II) with Imidazole-4,5-Dicarboxylate and 4,4'-Bipyridyl Building Blocks.

1
2
3 *Cryst. Growth Des.* **2006**, *6*, 564–571.
4
5

6
7 (61) Wang, Y. L.; Yuan, D. Q.; Bi, W. H.; Li, X.; Li, X. J.; Li, F.; Cao, R. Syntheses and
8
9
10 Characterizations of Two 3D Cobalt-Organic Frameworks from 2D Honeycomb Building
11
12
13
14 Blocks. *Cryst. Growth Des.* **2005**, *5*, 1849–1855.
15
16

17
18 (62) Beatty, A. M. Open-Framework Coordination Complexes from Hydrogen-Bonded
19
20
21
22 Networks: Toward Host/Guest Complexes. *Coord. Chem. Rev.* **2003**, *246*, 131–143.
23
24

25
26 (63) Zhang, J.; Xiong, R. G.; Chen, X. T.; Che, C. M.; Xue, Z.; You, X. Z. Two Luminescent
27
28
29
30 2D Layered Copper (I)-Olefin Coordination Polymers with High Thermal Stability.
31
32
33 *Organometallics* **2001**, *20*, 4118–4121.
34
35

36
37 (64) Hao, J.; Yu, B.; Hecke, K. Van; Cui, G. A Series of d¹⁰ Metal Coordination Polymers
38
39
40
41 Based on a Flexible Bis (2-Methylbenzimidazole) Ligand and Different Carboxylates:
42
43
44
45 Synthesis, Structures, Photoluminescence and Catalytic Properties. *CrystEngComm*
46
47
48 **2015**, *7*, 2279–2293.
49
50

51
52 (65) Abrahams, B. F.; Hoskins, B. F.; Michail, D. M.; Robson, R. Assembly of Porphyrin
53
54
55
56 Building Blocks into Network Structures with Large Channels. *Nature* **1994**, *369*, 727–
57
58
59

1
2
3 729.
4
5
6

7 (66) Dimos, A.; Tsaousis, D.; Michaelides, A.; Skoulika, S.; Golhen, S.; Ouahab, L.;

8
9
10 Didierjean, C.; Aubry, A. Microporous Rare Earth Coordination Polymers: Effect of

11
12
13 Lanthanide Contraction on Crystal Architecture and Porosity. *Chem. Mater.* **2002**, *14*,

14
15
16
17 2616–2622.
18

19
20
21 (67) Dhas, N. A.; Raj, C. P.; Gedanken, A. Synthesis, Characterization, and Properties of

22
23
24
25
26
27
28
29
30
31
32
33
34
35
36
37
38
39
40
41
42
43
44
45
46
47
48
49
50
51
52
53
54
55
56
57
58
59
60
Metallic Copper Nanoparticles. *Chem. Mater.* **1998**, *10*, 1446–1452.

(68) Boita, J.; Nicolao, L.; Alves, M. C. M.; Morais, J. Controlled Growth of Metallic Copper

Nanoparticles. *New J. Chem.* **2017**, *41*, 14478–14485.

(69) Kuzníková, L.; Dedková, K.; Pavelek, L.; Kupková, J.; Vána, R.; Rümmele, M. H.;

Kukutschová, J. *Synthesis and Characterization of Gadolinium Oxide Nanocrystallites*;

IntechOpen, 2016.

(70) Armaroli, N.; Accorsi, G.; Cardinali, F.; Listorti, A. Photochemistry and Photophysics of

Coordination Compounds: Copper. *Topics in Current Chemistry, Photochemistry and*

Photophysics of Coordination Compounds. 2007, pp 69–115.

- 1
2
3 (71) Xiong, Z.; Yuan, P.; Xie, Z.; Li, G. Three Transition-Metal Polymers from Imidazole
4
5
6 Dicarboxylates-Bearing Methoxyphenyl Groups: Syntheses, Crystal Structures and
7
8
9
10 Properties. *Supramol. Chem.* **2013**, *26*, 346–357.
11
12
13
14 (72) Manch, W.; Fernelius, W. C. The Structure and Spectra of Nickel(II) and Copper(II)
15
16
17 Complexes. *J. Chem. Educ.* **1961**, *38*, 192–201.
18
19
20
21
22 (73) Barbieri, A.; Accorsi, G.; Armaroli, N. Luminescent Complexes beyond the Platinum
23
24
25 Group: The d¹⁰ Avenue. *Chem. Commun.* **2008**, *19*, 2185–2193.
26
27
28
29
30 (74) Strasser, A.; Vogler, A.; Phosphorescence of gadolinium(III) chelates under ambient conditions,
31
32
33 *Inorg. Chim. Acta*, **2004**, *357*, 2345-2348.
34
35
36
37 (75) Bünzli, J.; Piguet, C. Taking Advantage of Luminescent Lanthanide Ions. *Chem. Soc.*
38
39
40 *Rev.* **2005**, *34*, 27-32.
41
42
43
44 (76) Cotton, S. Lanthanide and Actinide Chemistry; Interscience Publishers, John Wiley &
45
46
47 Sons 2006, pp 70.
48
49
50
51
52 (77) Feng, S.; Ma, L.; Feng, G.; Jiao, Y.; Zhu, M. Dinuclear Copper (II) Complexes Hold by
53
54
55 Crab-Shaped Pincer Ligands: Syntheses, Structures, Luminescent and Magnetic
56
57
58
59
60

1
2
3
4
5
6
7
8
9
10
11
12
13
14
15
16
17
18
19
20
21
22
23
24
25
26
27
28
29
30
31
32
33
34
35
36
37
38
39
40
41
42
43
44
45
46
47
48
49
50
51
52
53
54
55
56
57
58
59
60

Properties. *J. Chem. Struct.* **2014**, *1059*, 27–32.

- (78) Costes, J. P.; Dahan, F.; Dupuis, A.; Laurent, J. P. A Genuine Example of a Discrete Bimetallic (Cu, Gd) Complex: Structural Determination and Magnetic Properties. *Inorg. Chem.* **1996**, *35*, 2400–2402.
- (79) Koner, R.; Lee, G. H.; Wang, Y.; Wei, H. H.; Mohanta, S. Two New Diphenoxo-Bridged Discrete Dinuclear Cu^{II}Gd^{III} Compounds with Cyclic Diimino Moieties: Syntheses, Structures, and Magnetic Properties. *Eur. J. Inorg. Chem.* **2005**, 1500–1505.
- (80) Cañadillas-Delgado, L.; Fabelo, O.; Pasán, J.; Delgado, F. S.; Lloret, F.; Julve, M.; Ruiz-Pérez, C. Intramolecular Ferro- and Antiferromagnetic Interactions in Oxo-Carboxylate Bridged Digadolinium(III) Complexes. *Dalt. Trans.* **2010**, *39*, 7286.
- (81) Cañadillas-Delgado, L.; Pasan, J.; Fabelo, O.; Hernandez-Molina, M.; Lloret, F.; Julve, M.; Ruiz-Pérez, C. Two- and Three-Dimensional Networks of Gadolinium(III) with Dicarboxylate Ligands: Synthesis, Crystal Structure, and Magnetic Properties. *Inorg. Chem.* **2006**, *45*, 10585–10594.
- (82) Zhang, J.; Li, C.; Wang, J.; Zhu, M.; Li, L. Slow Magnetic Relaxation Behavior in Rare

Ln-Cu-Ln Linear Trinuclear Complexes. *Eur. J. Inorg. Chem.* **2016**, *2016*, 1383–1388.

(83) Winpenny, R. The Structures and Magnetic Properties of Complexes Containing 3d- and 4f-Metals. *Chem. Soc. Rev.* **1998**, *27*, 447.

(84) Hamamatsu, T.; Matsumoto, N.; Re, N.; Mrozinski, J. Chiral Ferromagnetic Chain of Copper(II)–Gadolinium(III) Complex. *Chem. Lett.* **2009**, *38*, 762–763.

(85) Benelli, C.; Caneschi, A.; Gatteschi, D.; Guillou, O.; Pardi, L. Synthesis, Crystal Structure, and Magnetic Properties of Tetranuclear Complexes Containing Exchange-Coupled Ln₂Cu₂ (Ln = Gd, Dy) Species. *Inorg. Chem.* **1990**, *29* (26), 1750–1755.

(86) Andruh, M.; Ramade, I.; Codjovi, E.; Guillou, O.; Kahn, O.; Trombe, J. C. Crystal Structure and Magnetic Properties of [Ln₂Cu₄] Hexanuclear Clusters Where Ln Mechanism of the Gd(III)-Cu(II) Magnetic Interaction. *J. Am. Chem. Soc.* **1993**, *115*, 1822–1829.

(87) Benelli, C.; Gatteschi, D. Magnetism of Lanthanides in Molecular Materials with Transition-Metal Ions and Organic Radicals. *Chem. Rev.* **2002**, *102*, 2369–2387.

- 1
2
3 (88) Cirera, J.; Ruiz, E. Exchange Coupling in Cu^{II}Gd^{III} dinuclear Complexes: A Theoretical
4
5
6 Perspective. *Comptes Rendus Chim.* **2008**, *11*, 1227–1234.
7
8
9
- 10 (89) Chen, X.M.; Wu, Y.L.; Aubin, S. M. J.; Hendrickson, D. N. Synthesis, Structures, and
11
12
13
14 Magnetic Properties of Carboxylate-Bridged Tetranuclear Copper(II)–Lanthanoid(III)
15
16
17
18 Complexes [Cu₂Ln₂(Betaine)₁₀(H₂O)₈](ClO₄)₁₀·2H₂O and
19
20
21 [Cu₂Ln₂(Betaine)₁₂(ClO₄)₂](ClO₄)₈. *Inorg. Chem.* **1998**, *37*, 6186–6191.
22
23
24
- 25 (90) Wu, B.; Zheng, Y.; Ng, S. W. Preparation, Structure and Magnetic Study of a New Linear
26
27
28
29 1-D Cu(II)–Gd(III) Coordination Polymer. *J. Coord. Chem.* **2008**, *61*, 3674–3678.
30
31
32
- 33 (91) Li, Y.; Zheng, F. K.; Zou, J. P.; Zou, W. Q.; Ma, H. W.; Guo, G. C.; Lu, C. Z.; Huang, J.
34
35
36
37 S. A Unique 3-D 3d-4f Heterometallic Coordination Polymer with Double Betaine Ligand:
38
39
40
41 Crystal Structure and Magnetic Properties. *Inorg. Chem. Commun.* **2007**, *10*, 787–791.
42
43
44
- 45 (92) Liu, S.; Song, W.; Xue, L.; Han, S.; Zeng, Y.; Wang, L.; Bu, X. Three New Cu(II)-Ln(III)
46
47
48
49 Heterometallic Coordination Polymers Constructed from Quinolinic Acid and Nicotinic
50
51
52
53
54
55
56
57
58
59
60 Acid: Synthesis, Structures, and Magnetic Properties. *Sci. China Chem.* **2012**, *55*, 1064–
1072.

- 1
2
3 (93) Zou, Y.; Yin, F.; Zhou, X. J.; Chen, J.; Meng, Q. J. A Cu^{II}-Gd^{III}-Cu^{II} Heterometallic
4
5
6 Coordination Polymer Constructed by Gadolinium(III) Ion and Copper(II) Schiff-Base
7
8
9
10 Building Block: Structure and Magnetic Property. *Inorg. Chem. Commun.* **2014**, *45*, 25–
11
12
13 29.
14
15
16
17
18
19
20
21
22
23
24
25
26
27
28
29
30
31
32
33
34
35
36
37
38
39
40
41
42
43
44
45
46
47
48
49
50
51
52
53
54
55
56
57
58
59
60

1
2
3
4
5
6
7
8
9
10
11
12
13
14
15
16
17
18
19
20
21
22
23
24
25
26
27
28
29
30
31
32
33
34
35
36
37
38
39
40
41
42
43
44
45
46
47
48
49
50
51
52
53
54
55
56
57
58
59
60

For Table of Contents Use Only

*Carlos Cruz,^{a,b} Francisco Rubio^{a,b} Diego Venegas-Yazigi,^{b,c} Nathalie Audebrand,^d Christophe Calers,^d Evgenia Spodine^{b,e} and Verónica Paredes-García^{*a,b}*

^a Universidad Andrés Bello, Facultad de Ciencias Exactas, Departamento de Ciencias Químicas, Santiago, Chile.

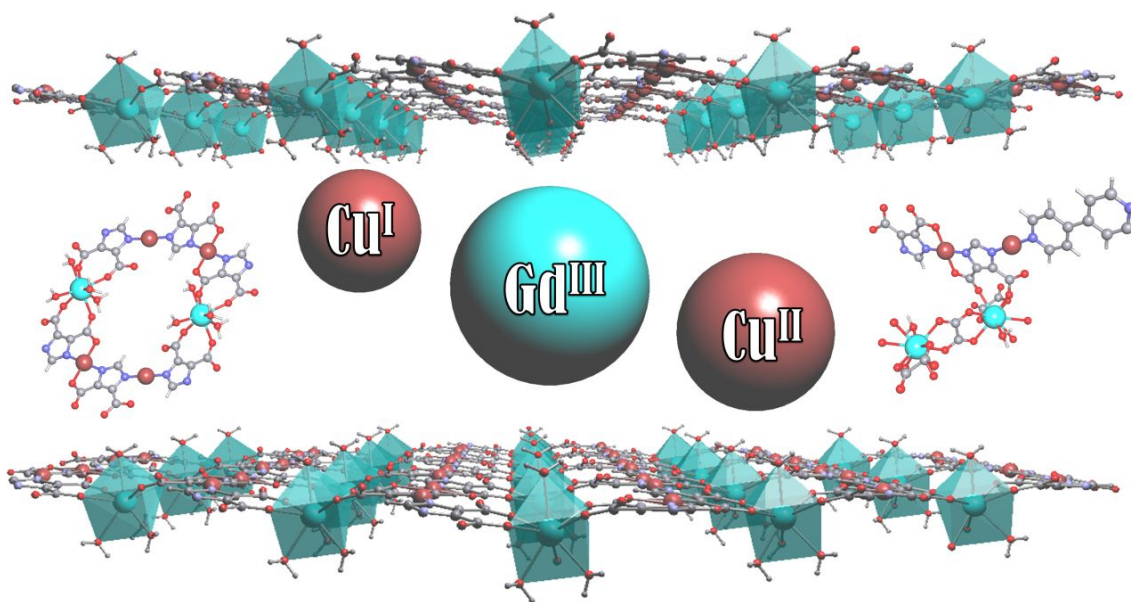
^b CEDENNA, Santiago, Chile.

^c Universidad de Santiago de Chile, Facultad de Química y Biología, Departamento de Ciencias de los Materiales, Santiago, Chile

^d Univ Rennes, CNRS, ISCR (Institut des Sciences Chimiques de Rennes) - UMR 6226, F-35000 Rennes, France

^e Universidad de Chile, Facultad de Ciencias Químicas y Farmacéuticas, Departamento de Química Inorgánica y Analítica, Santiago, Chile.

TOC graphic



Synopsis

24 Two new Cu^I/Cu^{II}-Gd^{III} mixed valence heterometallic coordination polymers are reported,
25 [Gd(H₂O)₄Cu^{II}Cu^I(IDC)₂] **1** and [Gd₂(H₂O)₂(C₂O₄)₂Cu^{II}(IDC)₂Cu^I₂(4,4'-bipy)]·4.5H₂O **2**. Compound **1**
26 present a 2D honeycomb network constructed by a single organic linker (IDC³⁻) while **2** present a 3D
27 structure with three different organic ligands (IDC³⁻, C₂O₄²⁻ and 4,4'-bipy). Both **1** and **2** exhibit
28 ferromagnetic interactions below 50 K.
29
30
31
32
33
34
35
36
37
38
39
40
41
42
43
44
45
46
47
48
49
50
51
52
53
54
55
56
57
58
59
60